DESIGN AND MANUFACTURE OF AN ENGINEERED SURF FOIL

by

Todd Backus

Jackson Bryla

Anthony Taylor

Report Presented to the

British Columbia Institute of Technology (BCIT)

In partial fulfilment of the requirement for the degree of

Bachelor of Engineering (Mechanical)

Faculty Advisors: Johan Fourie

Greg King

Program Head: Mehrzad Tabatabain

Burnaby, British Columbia, Canada, 2019

Author's Declaration

We hereby declare that we are the sole authors of this report.

Todd Backus   Jackson Bryla   Anthony Taylor

We further authorize the British Columbia Institute of Technology to distribute digitally, or printed paper, copies of this report, in total or in part, at the request of other institutions or individuals for the purpose of scholarly activity.

Todd Backus   Jackson Bryla   Anthony Taylor

Abstract

The surf foil system detailed herein was designed at the request of Poseidon Adventures Ltd. Included in this publication are links to the part models and STL files for all of the components that were designed for the surf foil system.

The component parts that were designed for prototyping are both wings, the mast, and the fuselage of the surf foil. The front wing has a span of 32", the rear wing has a span of 16" and they are roughly 1" thick. The fuselage is 30" long and is made from 1" dia. aluminum rod. The manufacture of the fuselage and both wings were completed. A mast was purchased for the assembly of the product for final presentation due to time restrictions. The design of the mast is complete, its manufacture is ongoing at the date of this report's publication. The overall weight of the surf foil system including the purchased mast, mast pedestal, and board mount is 8 lbs.

An emphasis was placed on using standard dimensions whenever possible so that commercially available parts could be used as a replacement for an individual component in the event of a catastrophic failure.

Reproduction of the surf foil is possible but be mindful of careless operation of this device. This sport is dangerous, so use it at your own peril. Head protection and life vests are always recommended, as well as protection of the eyes.

Acknowledgements

The authors would like to thank their project advisors, Johan Fourie and Greg King, for helping to ensure this project was educational, fun, and rewarding. Their excitement about this project was apparent from the start and that has made the project all the more worthwhile.

They would also like to thank:

Casey Keulen, whose expertise with composite materials guided them through the tricky work of manufacturing with carbon fibre and epoxy;

Chris Chambers, for his support, enthusiasm, and advice on foils and manufacturing. Chris is a kite-foiling enthusiast from BCIT's TTED program, whom saw the potential of the project and was so happy with the results that he has built and will be testing his own copy of the surf foil described herein;

Chris Townsend, for his help and guidance in manufacturing the fuselage, for teaching them how to use the milling machine, and for providing access to the shop.

Adam Marciniak for his help with Python coding.

The faculty at BCIT for sharing their knowledge and providing support throughout the project.

Contents

List of Tables

Table of Figures

1 Introduction

The Request for Proposal (RFP) issued by Poseidon Adventures, included in Appendix A "Original Request for Proposal (RFP)", detailed the need for a surf foil that could compete with the current commercially available products, be manufactured on a scale of 30 units per month and not be cost prohibitive.

There is a wide range in the sophistication of design in the surf foil market. While there are high-end manufacturers who employ engineering techniques to design their products, the prevailing trend employed by many smaller companies in the industry is a trial and error process. The objective of this project was to design a surf foil system that would satisfy the requirements set out in the RFP and employ engineering knowledge to explain the behaviour of the designed product.

Given the popularity of water sports in North America, there are 11 million water skiers in the United States alone [1], the product was designed with the average North American user in mind. Given that the average weight of an American male over 20 years of age is 197 lbs [2], this was considered as the design weight for a rider.

Final product weight is an important consideration in the design to ensure the hydrofoil can be easily carried by users as well as prevent the introduction of a significant amount of weight to the board-rider system. To help achieve a low weight for the final product, light-weight aluminum extrusions and woven carbon fibre composite materials were selected for use in the design.

To create a light-weight core for the composite front and rear wings, additive manufacturing was employed. A 3D-printed Polylactic acid (PLA) plastic core was used as a base to layup a carbon-fibre epoxy composite. The fuselage is made of a 1” dia. 6061-T6 aluminum round stock that has been machined, hand filed, and powder-coated. The fuselage was designed to interface with several standard masts and wing dimensions for the purpose of modularity and ease of component replacement. A mast was designed using a similar approach to the front and rear wings (e.g. PLA core with carbon-fibre epoxy composite layup), except for the addition of aluminum cores for strength and to allow the mast to be securely fastened to the board and fuselage. The aluminum cores were added into the design because the mast in a surf foil needs to withstand a large amount of bending stress which the non-structural PLA core is not able to reliably withstand alone. Due to time constraints the designed mast was not manufactured, but a commercially available set of 18”, 24”, and 30” masts were purchased from SlingShot® in order to ensure project completion. The modeled wings, mast, and fuselage are shown in Figure 1.1. Figure 1.2, on the next page, shows the as-built prototype attached to a Slingshot mast.

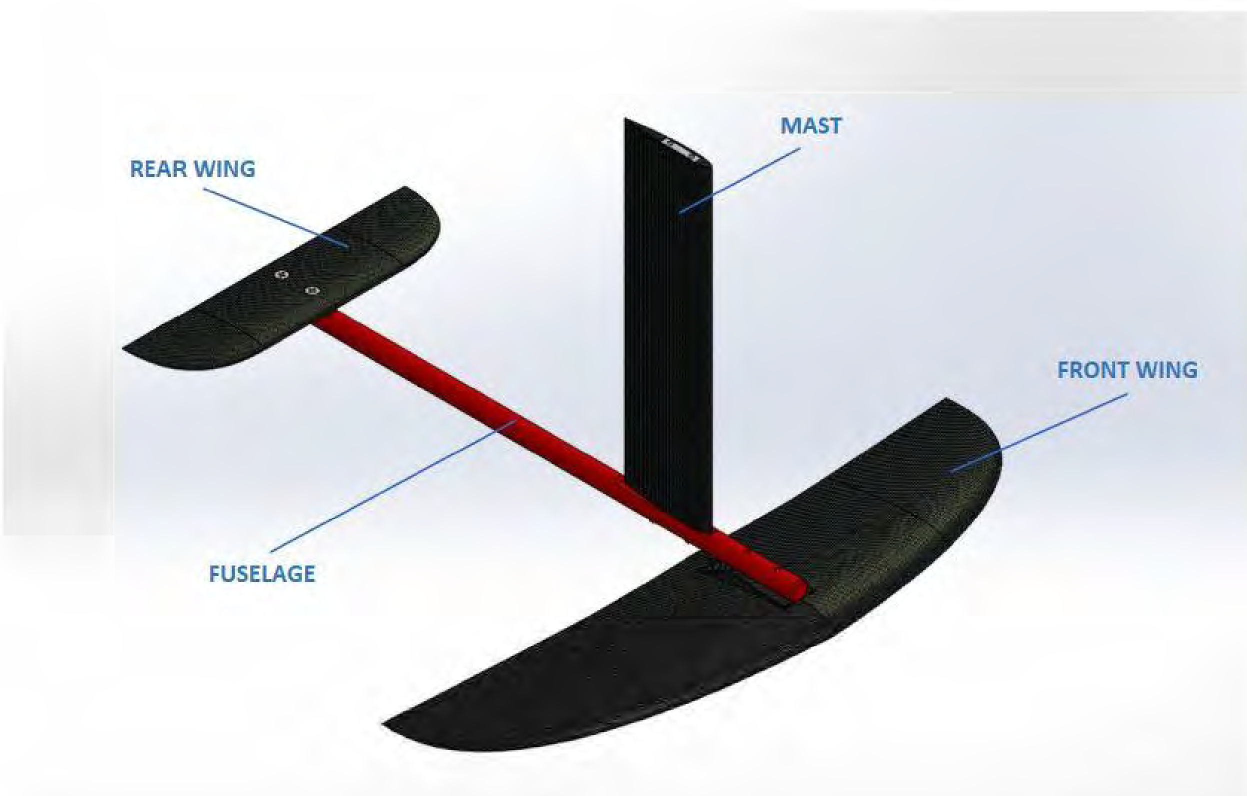

Figure 1.1: Surf Foil Assembly Model with Labels

Figure 1.2: Fully Manufacture Surf Foil System

The finalized SolidWorks® part files, as well as the STL files, used by 3D printing software, are linked to this document. It is the hope of the authors that others will use these files to create their own surf foils projects, they are provided in good faith that they will not be used for commercial purposes and are used responsibly. The authors and BCIT assume no responsibility for any injuries or damage suffered through the use of, or attempt at reproducing, this product.

Alterations to the files are permitted, at the user's risk, so long as the results are not used for commercial purposes.

Surf Foiling is a dangerous sport, safety equipment such as helmets, personal flotation devices and goggles should always be worn by riders.

1.1 Projected Product Capabilities

Based on lift calculations [See Appendix B], the following design should be able to lift a 198lb person at a velocity of approximately 10mph, which were the requirements identified during the design review [Appendix C]. A low foiling velocity is desired to maximize the acceptable outdoor conditions for the surf foil to be used. It is possible that an experienced rider could start foiling from the velocity generated by surfing a medium wave. However; this is dependent on the board that the foil is attached to and outdoor conditions. Other methods of propulsion may include towing by boat or by kite. The product was designed to accommodate the surfer with a wide range of operational velocities with good overall stability so that they can enjoy its use in as many different situations as possible.

2 Background & Research

The surf foil industry is relatively new but major competitors have emerged and hold significant stakes of the market. Inspiration for BTB's design came from independent makers, hobbyists, as well as industry leaders such as SlingShot, Cabrinha, Naish and Takuma foil manufacturers.

2.1 Independent Surf Foil Design and Manufacture

Independent surf foil makers are an excellent resource for designs that are robust and easy to manufacture [3]. The deficiency in the design of many of these recreational foils is due to the lack of knowledge in fundamental fluid dynamics as well as access to sophisticated and precise machining equipment. The surf foil design featured for Seabreeze [Figure 2.1] has a fixed mast and fuselage, this is due to the core material being manufactured from plywood. This approach was avoided by the team due to the lack of modularity that is inherent in a mast and fuselage system that are not detachable. Any failure in the section results in the destruction of both mast and fuselage. The shaping of the wooden members is time consuming and requires a considerable level of machining experience to achieve a professional finished product. Concerns about water ingress into a wooden core was another issue identified with this design.

Figure 2.1: Seabreeze Surf Foil [4]

2.2 Professional Surf Foil Design and Manufacture

Most commercial surf foil manufacturers do not disclose the composition of their cores. There are several possible candidates for core material, such as plastic or foam, which are likely the most commonly used in industry. A foam core was considered due to the ease of shaping and the additional buoyancy that it would provide but was ruled out due to the difficulty in mounting the wings to the fuselage while providing adequate crush protection around the fasteners. The use of a foam core for the wings is feasible as professional manufacturers such as Naish are already using this method [5].

The use of plastic PLA formed by additive manufacturing is an excellent application of this technology. The structure of the core should be light to reduce overall weight, which can be achieved by using a low percentage infill. The printing of the wing also allowed for a more complex design without requiring extensive machining experience and skill.

Carbon fibre and epoxy composites are common for high-quality custom-built surf foil wings. Masts are typically either carbon fibre and epoxy composite or aluminum [6]. The cost savings of the aluminum mast are significant but the carbon fibre mast yielder higher performance, primarily due to the weight reduction. Carbon fibre masts are typically not recommended for learning because of the high cost. The pendulum effect caused by the length of the mast is a significant challenge in terms of muscle control of the rider, resulting in a lack of control and stability. Purchasing an aluminum mast set is advised, as the rider becomes more experienced, they move on to taller masts. A typical starting mast length is 18", expert riders will ride masts up to 48" in length [7].

2.3 Design and Performance Parameters Overview

There are many styles and designs of foils due to the different requirements of foil-sport customers. For example, stand-up paddle boards (SUP) would typically have large wings capable of providing lift at low velocities, whereas kite boards would employ a smaller more maneuverable wing suited to their high velocities.

The surf foil was designed to be mounted to a wake surf board and then towed by a boat. Other methods are propulsion are available, such as having the surf foil attached to a kite board and propelled by wind energy through a sail or a large kite.

The operational velocity range for different foil applications varies significantly. For a given wing area, higher velocities provide lift more readily than lower velocities, it follows that the intended use of the surf foil was therefore a key factor in designing the shape and size of the wings. The wing size and shape dramatically affect the performance of the system, particularly in the case of ride stability, operational foiling velocities, and maneuverability. For this application, maneuverability and agility was favoured over stability. In order to be more user-friendly; sufficient lift for foiling needed to occur at approximately 11 mph. Maneuverability was favored over stability with the aim of having a more thrilling rider experience.

The following sub-sections details the corresponding design and performance parameters. These parameters describe the relationships between design inputs, foil performance outputs, and any trade-offs that must be made when balancing the user requirements with design constraints. For example, an increased wing surface area achieves greater lift but also increases drag forces. A quick overview of the relationship between the performance parameters and the design parameters are provided below in Table 2.1.

2.4 Design Parameters vs Performance Parameters

Table 2.1: Relationship between performance and design parameters.

Design Parameters	Performance Parameters	Correlation
Fuselage Length	Pitch Stability	+
	Yaw Stability	+
Mast Length	Yaw Stability	-
	Roll Stability	-
	Max Operational Velocity	+
Front Wing Aspect Ratio: Top	Max Operational Velocity	+
	Lift / Speed	-
	Lift : Drag Ratio	-
	Max Weight of User	-
Front Wing Aspect Ratio: Side	Lift : Drag Ratio	+
	Max Weight of User	+
Rear Wing Aspect Ratio: Top	Pitch Stability	-
	Roll Stability	+
Rear Wing Aspect Ratio: Side	Pitch Stability	+
Vertical Fins	Yaw Stability	+
	Roll Stability	+
Anhedral Wing	Roll Stability	-
Dihedral Wing	Roll Stability	-
Total Wing Surface Area	Max Operational Velocity	+
	Max Operational Velocity	-
	Lift / Speed	+
	Lift : Drag Ratio	+
	Roll Stability	+
Angle of Attack	Lift : Drag Ratio	+
	Max Weight of User	+

Positive Correlation (+): Increase in design parameter results in increase of the performance parameter
Negative Correlation (-): Increase in design parameter results in decrease of the performance parameter

2.4.1 Wing Shape

An anhedral wing is shaped with a downwards slope from the fuselage, as shown in the lower right image (b) of Figure 2.2. Conversely, a dihedral wing is one that slopes upwards from the fuselage, as seen in the lower left image (a) of Figure 2.2.

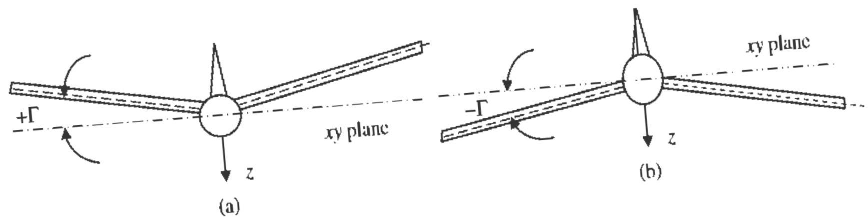

Figure 2.2: Effect of Dihedral and Anhedral Angles [8].

The wing is mounted below the board in the water, which causes the system to act similarly to a pendulum due to the length of the mass. This is critical to the performance parameter of roll stability, (see

Figure 2.3 for explanation of roll, pitch, and yaw).

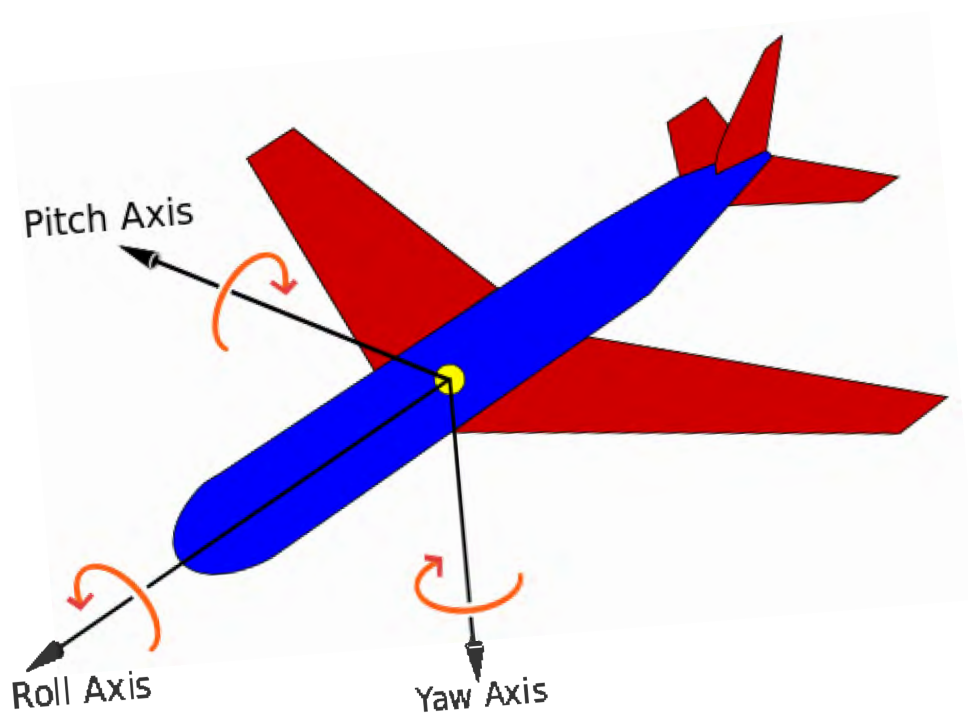

Figure 2.3: Orientation of Roll, Pitch, and Yaw [9]

For the intended performance of the designed surf foil, an anhedral front wing was desirable for increased maneuverability. This allows turns to be performed more easily, making movement along the wake easier. In addition, the anhedral shape assists with foiling at lower speeds, which is particularly helpful for novice riders [10].

The anhedral wing adds yaw stability due to the fact that when viewed from the side, it has a vertical wing area which helps direct fluid flow over the system [11]. An anhedral front wing is less prone to breaching the surface when banking the board over its rolling axis. This is desirable as breaching the water with a wing will often result in a crash.

A drawback of the anhedral wing is the reduction of overall roll stability. Because the anhedral shape amplifies the turning input, the board is more likely to flip over, particularly when used in conjunction with a long mast. This shape does reduce the maximum operating speed [10] but that is not a significant drawback as the maximum velocity is well outside the range of comfort for most riders.

An anhedral rear wing decreases the pitch stability of the system. This effect is not as dramatic as increasing the anhedral angle of the front wing due to the rear wing having a significantly smaller surface area compared to the front wing. [10]

Figure 2.4: An example of a dihedral front wing. [12]

In contrast, a dihedral wing is one that is upswept over the pitch axis, shown above in Figure 2.4.

Dihedral front wings are common in stand-up paddle (SUP) foil design as they are inherently more stable than anhedral wings with respect to rolling [11]. This is due to the dihedral angle introducing a restoring moment which will oppose a rolling motion generated by the rider which is required to turn the board. Dihedral wings will not be considered further as the reduction in maneuverability is contrary to the desired performance of this projects design.

2.4.2 Wing Sweep

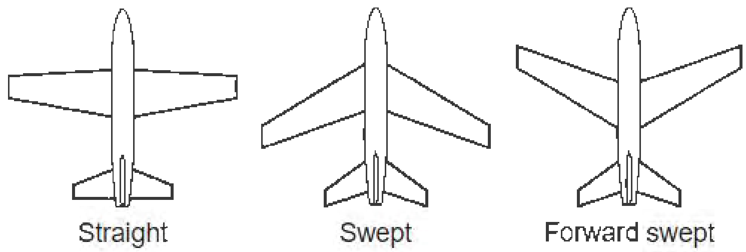

Figure 2.5: Wing Sweep Configuration Examples [10]

Wing sweep refers to the direction that the wing is projected from the fuselage when viewed from above. This is displayed in Figure 2.5. A wing can be backswept, delta, forward swept, or straight each with their own advantages and drawbacks. Performance of the forward and backwards swept wings will be compared to straight wings as a baseline.

Forward swept wings are known to have higher maneuverability. They also create more lift than comparable sized backswept wings by directing wingtip vortices from the wingtips to the fuselage [13]. Forward swept wings create drag when experiencing yaw (one wingtip is farther forward than the other) and this drag amplifies the yaw movement [13]. This feedback is undesirable for this surf foil design because there is no purpose-built vertical wing to resist yaw motion, the design relies upon the mast and vertical projections of the anhedral front wing to resist and stabilize yaw.

Delta wings can be made stiffer than swept wings as their root (inboard) chord length is typically longer. A common problem with delta wing aircraft is that they are prone to stalling at steep attack angles [14]. This is undesirable as stalling the surf foil will result in a crash.

Backwards swept wings are easier to recover from a stall than forward swept wings [13] but are more prone to stalls than forward swept wings [15].

Stalling with a foil will be a non-issue because the wing will not be able to reach stall angles without breaching the water. A backwards swept wing was chosen for aesthetics, ease of manufacturing, and the reduction of drag forces.

2.4.3 Mean Chord Length: Wings

The mean chord length is the centerline length of the wing, measured from the leading edge to the trailing edge of the wing. For symmetrical profiles [Figure 2.7**Error! Reference source not found.**] the chord length is the length of the horizontal line drawn from front to back on the wing. For wings that have asymmetrical profile, the camber line is a curve.

2.4.4 Chord Variation along Wingspan

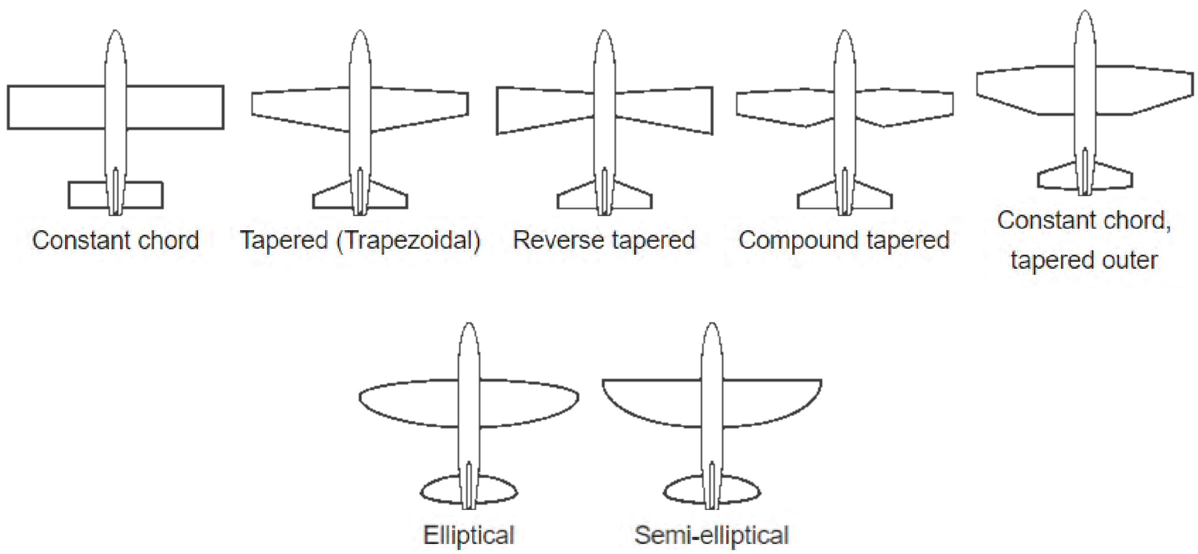

Figure 2.6: Chord Variation along Wingspan [15]

As seen in Figure 2.6, a wings chord can vary along its wingspan. Chord variation along the wingspan directly relates to the wing surface area and thus to lift. For example, an elliptical wing is able to generate more lift than a constant chord wing and it saves weight at the wing tip [15].

For this project the front wing has a leading edge that resembles a tapered wing generated from a Bezier curve to create an elliptical leading edge. The rear wing is semi-elliptical using a Bezier curve to provide a high surface area to weight ratio.

2.4.5 Aspect Ratio - Side View

The side view aspect ratio is the ratio of cross-sectional area to mean chord length. The lift force is affected by changes to this parameter through the equation:

$$F_L = \int_0^c \Delta P_l \cos\beta_l - \Delta P_u \cos\beta_u$$

[Eqn. 1]

Where β represents the angle of the slope of the wing surface at some position along the chord for the upper and lower surface [16].

If area is fixed and the length is changed, then the slopes (β) change which alters the resulting lift force.

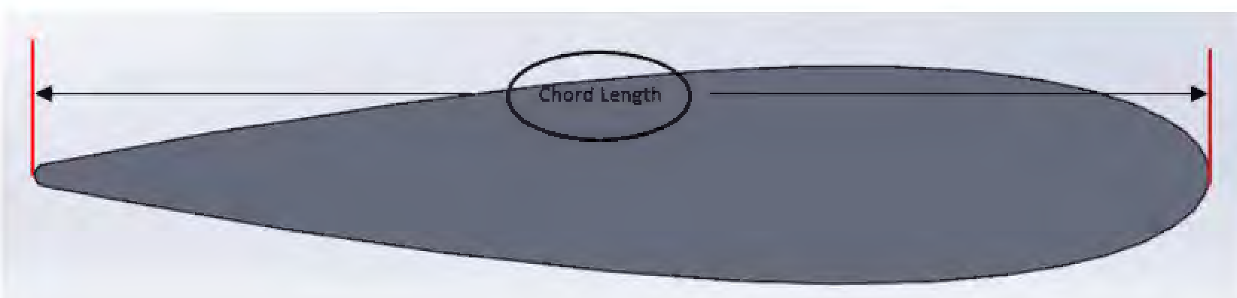

Figure 2.7: Cross Section of NACA 0018 Wing Profile - Side View.

Increasing the aspect ratio of the front wing (viewed from the side) will result in an increase in the maximum allowable operational weight because it produces greater lift. [17].

The plan view aspect ratio is the ratio of wing span to mean chord length.

In addition to the formula shown above, the lift force can be calculated by:

$$F_L = C_L \frac{\rho}{2} V^2 SA$$

[16]

As the surface area of the wing increases the lift force also increases.

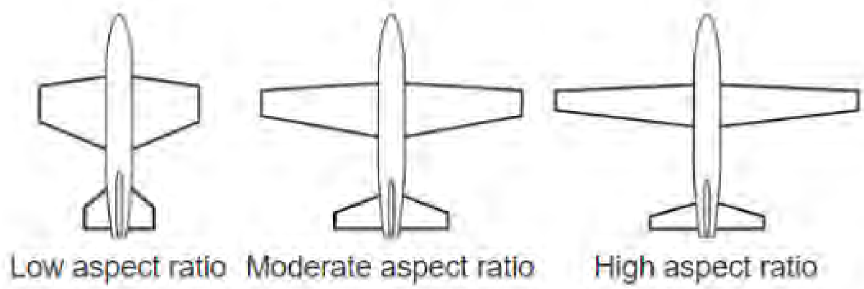

Figure 2.8: Wing Aspect Ratios [15]

Low aspect ratio wings are more structurally efficient whereas, high aspect ratio wings are more aerodynamically efficient [15].

2.4.6 Total Surface Area: Drag and Lift

In traditional aircraft design, the main function of the front wing is to provide lift for flight, while the main function of the rear wings, is to provide flight stability, namely pitch stability. [18] For this reason, their size, and therefore surface areas differ significantly.

Lift is the result of air travelling over the top and bottom surfaces of a wing at different speeds. According to Bernoulli's principle, velocity and pressure are inversely proportional. On a wing, when air travels faster over the top surface than the bottom surface, a pressure differential is established, and the wing experience a force exerted in the direction of high to low pressure. This is shown in Figure 2.9.

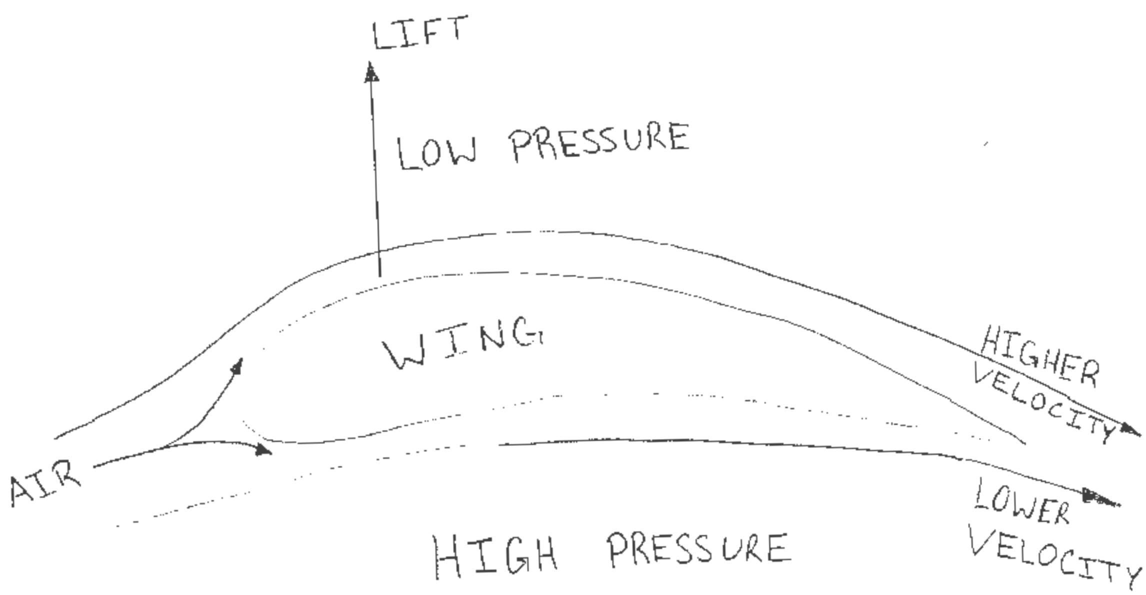

Figure 2.9: Bernoulli's Principle Applied to Wing Lift

Lift surface area and is defined by the following equation:

$$L = \frac{1}{2}\, C_l\, \rho v^2 A_s \qquad \text{[Eqn. 2]}$$

Where C_l is the lift coefficient, ρ is the fluid density, v is the fluid velocity, and A_s is the surface area over which the fluid flows [19]. Lift is directly proportional to wing surface area. The front wing should have a large surface area because their main function is to produce lift.

The rear wing also produces lift but in a downwards direction (i.e. a tail down force) which balances the moment about the centre of gravity produced by front wing. The foil will comprise less than 10% of the board-rider mass, so it was assumed that the center of gravity of the system would be forward of the mast. The case shown in Figure 2.10 is representative of the force directions desired for a surf foil.

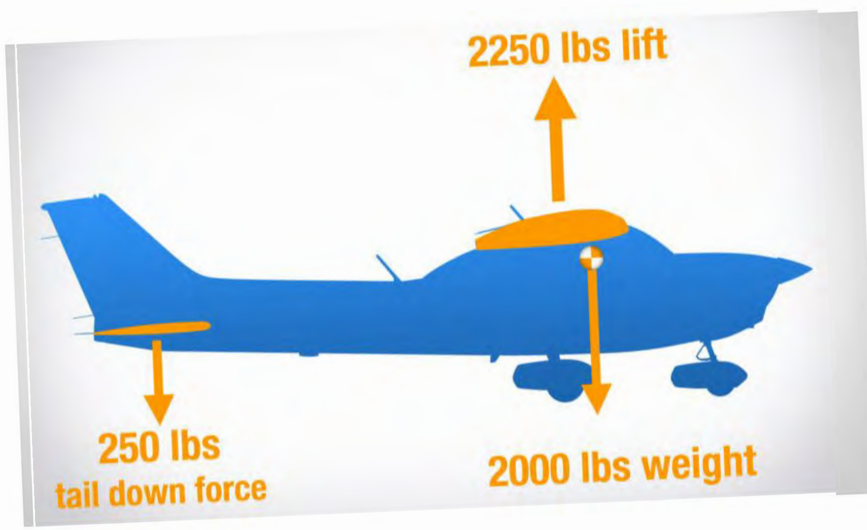

Figure 2.10: Lift Forces on a Plane [15].

Drag is a resistive force exerted on an object travelling through a medium, it is directly correlated to surface area. Drag between a body in a moving fluid is defined by the following equation:

$$D = \tfrac{1}{2}\, C_d\, \rho v^2 A_{ref} \text{ [20]} \qquad \text{[Eqn. 3]}$$

Where C_d is the drag coefficient, ρ is the fluid density, v is the fluid velocity, and A_{ref} is the reference area. [21] The reference area changes depending on whether drag caused by resistance to flow (i.e. form drag) or friction between the fluid and wing surface (i.e. skin friction). Drag due to skin friction depends on the total surface area, where form drag depends on the projected area perpendicular to the direction of flow [20]. This section pertains to skin friction; for more information on form drag see the below section on angle of attack.

As seen in the above equation, the drag force generated is directly proportional to the area of the body for a given set of fluid properties and conditions. If the surface area is doubled, so is the drag due to skin friction.

To achieve an efficient wing design in terms operational velocity range, the selection of a NACA profile with a high lift to drag ratio was required.

2.4.7 Fuselage Length & Size

The fuselage is a central member that joins both wings and the mast together. The length of the fuselage determines the location of the front and rear wing with respect to each other as well as where the wings ultimately rest under the board.

In an aircraft, the forces exerted on the wings induce a pitching moment about the center of gravity. Given that a surf foil is attached to a mast, the mast connection point can be thought of as the center of gravity for the wing-fuselage-mast system. An example of forces exerted on a fuselage by wings is shown in Figure 2.11.

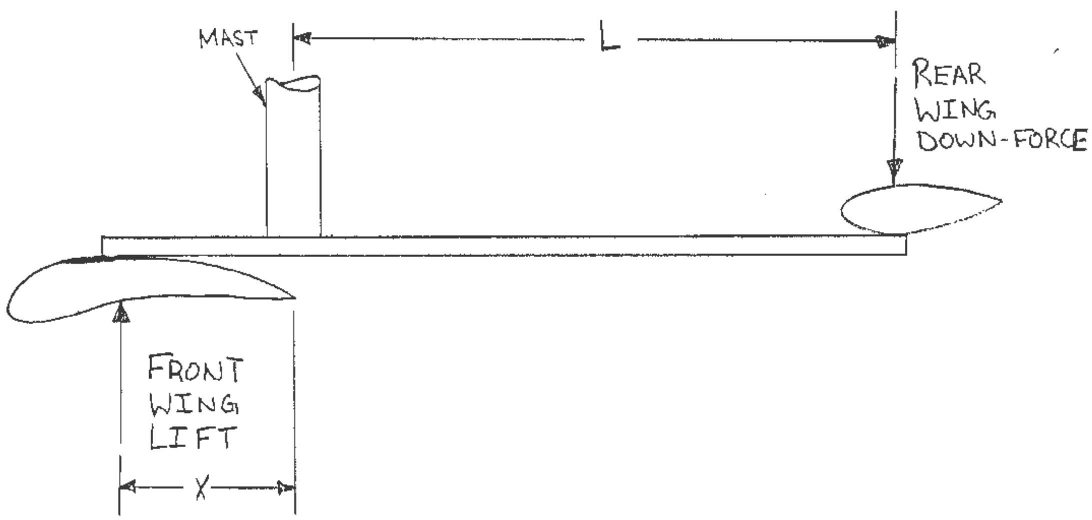

Figure 2.11: Force Directions Acting on the Fuselage

For a surf foil that employs a front wing with upwards lift and a rear wing with downwards lift, a clockwise moment is induced about the mast connection point. This moment is counteracted by the rider shifting their weight distribution forward or backward as needed.

A thick fuselage will introduce more drag to the hydrofoil, decreasing the maximum operation velocity and increasing the amount of applied force required for motion. The thickness of the fuselage is determined by the maximum allowable yield strength of the material that is required to prevent critical failure.

2.4.8 Mast Chord Length

Typically, the chord length of the mast is around 4in.The thickness of the mass is dependent on the required strength and stiffness of the design. A lack of stiffness in this member will significantly decrease the yaw, pitch, and roll stability, which decreases the overall maneuverability of the surf foil. Decreasingly the chord length requires an increase in mast thickness to preserve the member's strength. Decreasing this aspect ratio will alter the shape factor which results in generating more drag force and decreasing maneuverability [10].

2.4.9 Mast Length

A long mast allows the surfer to rise higher out of the water, lifting the board above the chop but it also decreases roll stability by creating a greater pendulum effect due to the mass of the foil at the end of the mast. Short masts are recommended for novice riders as they are easier to control. Long masts are used in racing as they provide a smoother ride across large waves, cruising above the chop and, in the case of a kiteboard, a better upwind angle can be used [22]. A typical progression of mast lengths are shown in Figure 2.12.

Figure 2.12: Masts of different length [23].

2.4.10 Angle of Attack

As the foil moves through water, the centerline of the wings are often not perpendicular to the velocity, but rather at some inclined angle. This angle is referred to as the angle of attack. The effect of the angle of attack is a change in fluid speed over the wing surface. This results in a change in pressure and lift as depicted in Figure 2.13.

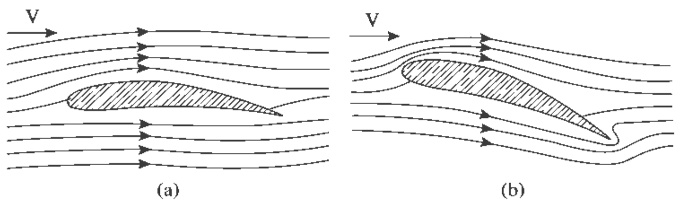

Figure 5.6 Flow around an airfoil: (a) Small angle of attack; (b) Large angle of attack

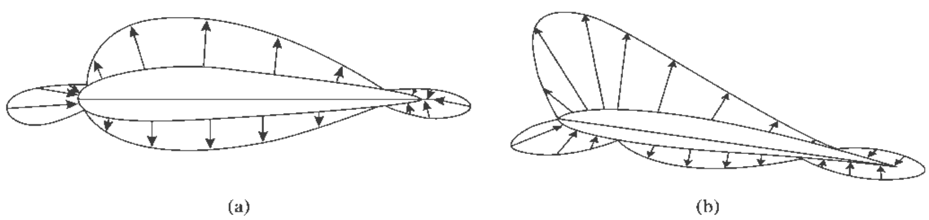

Figure 2.13: Pressure Distribution of an Inclined and Non-Inclined Airfoil [8]

Depending on the projected area and shape of the wing, a considerable increase in the amount of lift is generated as the angle of attack is increased, as is shown in Figure 2.14. As a result of the increased lift, the effects of drag resistance to fluid motion (not frictional drag) is generated. At too great an angle, the flow becomes separated and stalls, which would almost certainly cause the rider to crash. Predicting the stall point is difficult to determine by calculation due to the complexity of the wing geometry and is therefore typically determined through experimentation [24]. Although the increase in the angle of attack will create more lift, increasing the angle beyond 15° typically leads to diminishing returns.

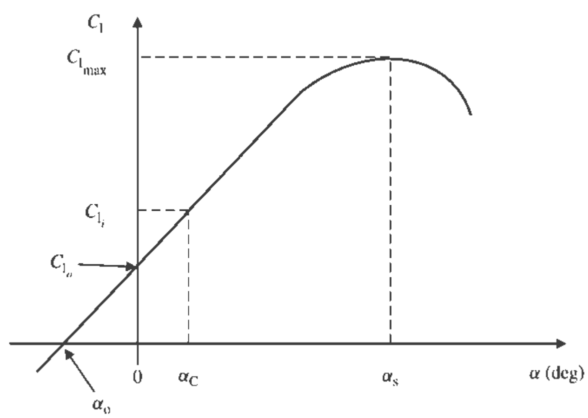

Figure 5.11 The variations of lift coefficient versus angle of attack

Figure 2.14: Lift Coefficient vs. Angle of Attack [8]

3 Description of the Project Activity and Equipment

3.1 Component Design

3.1.1 Wing Design

The overall size and shape of the wings are heavily influenced by the design specifications mentioned in the request for proposal [Appendix A], primarily the minimum and maximum foiling velocity of approximately 18.8 km/h and 32.3 km/h, respectively, as well as the prescribed load of 90kg.

The NACA 23015 airfoil shape, shown in Figure 3.1, was selected for both front and rear wings due to the asymmetrical cross section, the excellent lift to drag ratio, and the relative stability during small changes to attack angle. The profile of the rear wing is opposite to the front wings as the front wing provides positive lift and the rear wing provides negative lift. The high lift to drag ratio of the wings are complemented by a high aspect ratio with respect to the plan view of the wing. This decreases structural efficiency but significantly increases the aerodynamic efficiency [15].

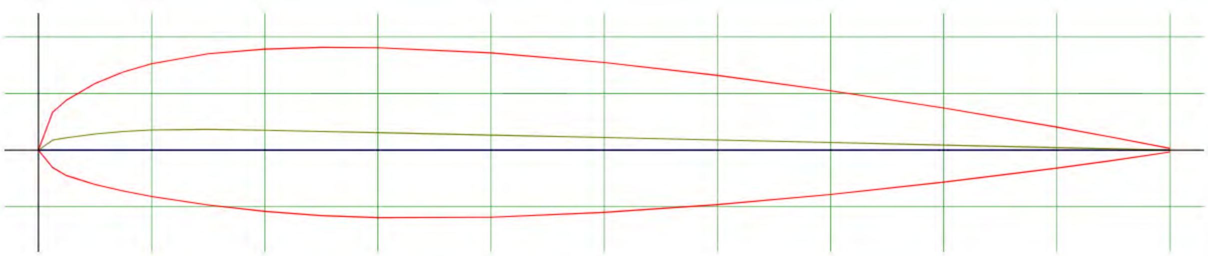

Figure 3.1: Profile of the NACA 23015 Airfoil [25]

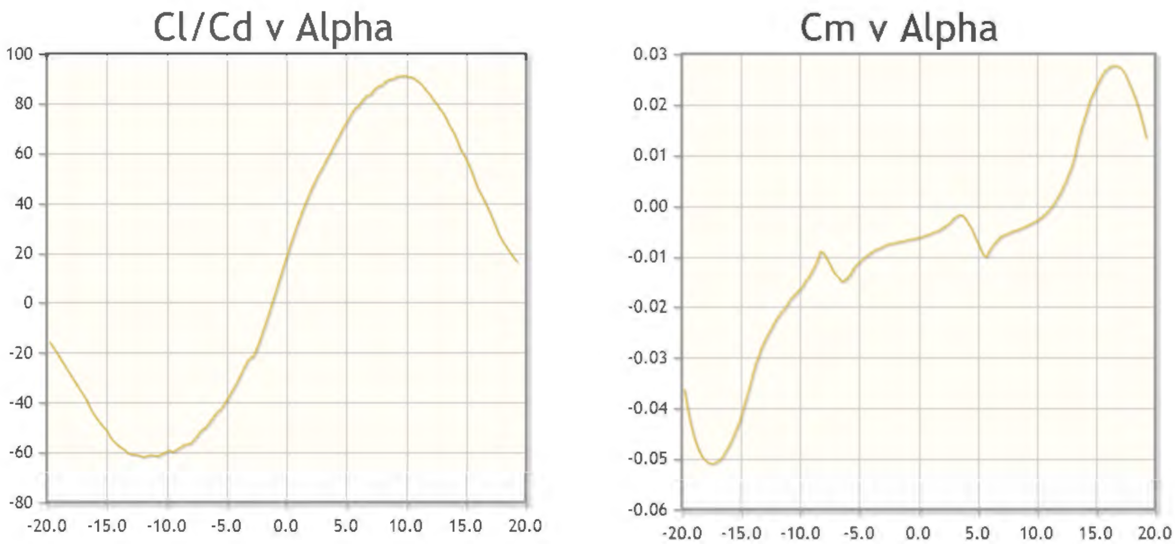

Figure 3.2: (L): Lift/Drag Ratio vs. Attack Angle, (R): Internal Moment Coefficient vs. Attack Angle

The website outputs the curves shown above in Figure 3.2 for each foil shape that was considered.

After selecting the NACA wing profile, analysis using the program XFOIL (version 6.99 [26]) was done to achieve a better understanding of the pressure distribution on the wing profile. Below in Figure 3.3, is the output from XFOIL showing the pressure distribution over the cross-section of the airfoil on the right, and a graphical representation of the pressure coefficient on the left.

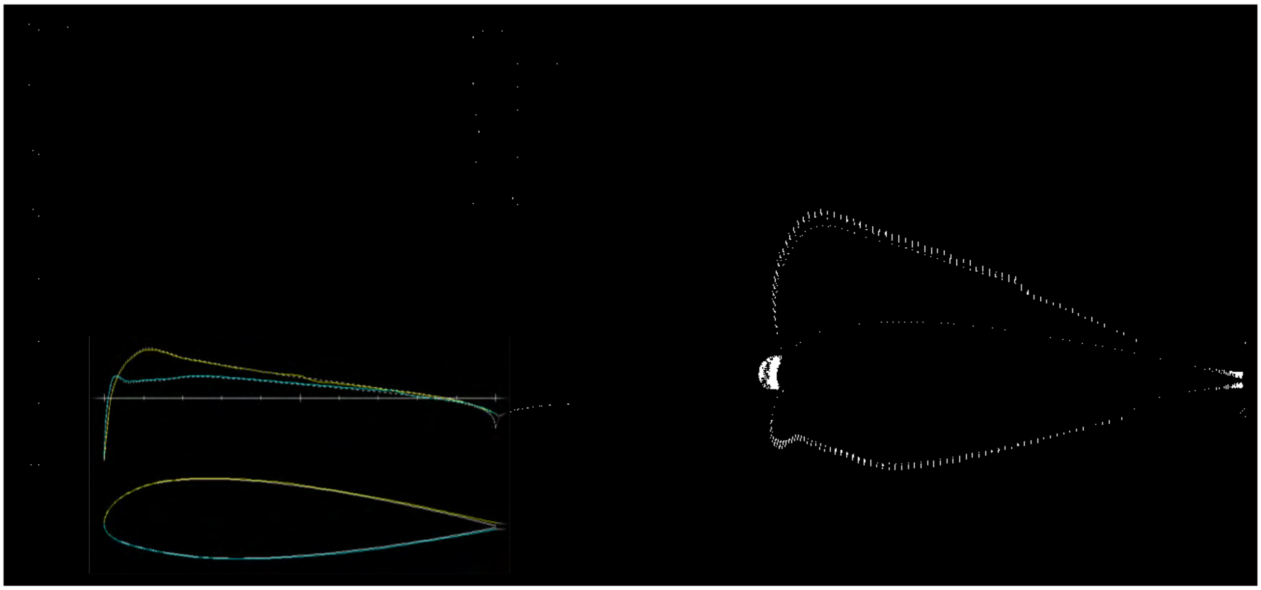

Figure 3.3: Pressure Distribution on NACA 23015 – XFOIL

This particular simulation was performed using the parameters shown below in Table 3.1.

Table 3.1: Parameters for XFOIL Simulation

Parameter	Reynold's Number	Angle of attack	Flow Type
Value	8.00E+05	0	Viscous

In order to estimate an appropriate Reynold's number for the simulation, an estimate of 10°C for the water temperature for Vancouver, Canada was calculated by using the sea temperature readings collected from the National Oceanic and Atmospheric Administration (NOAA) satellite, shown below in Figure 3.4.

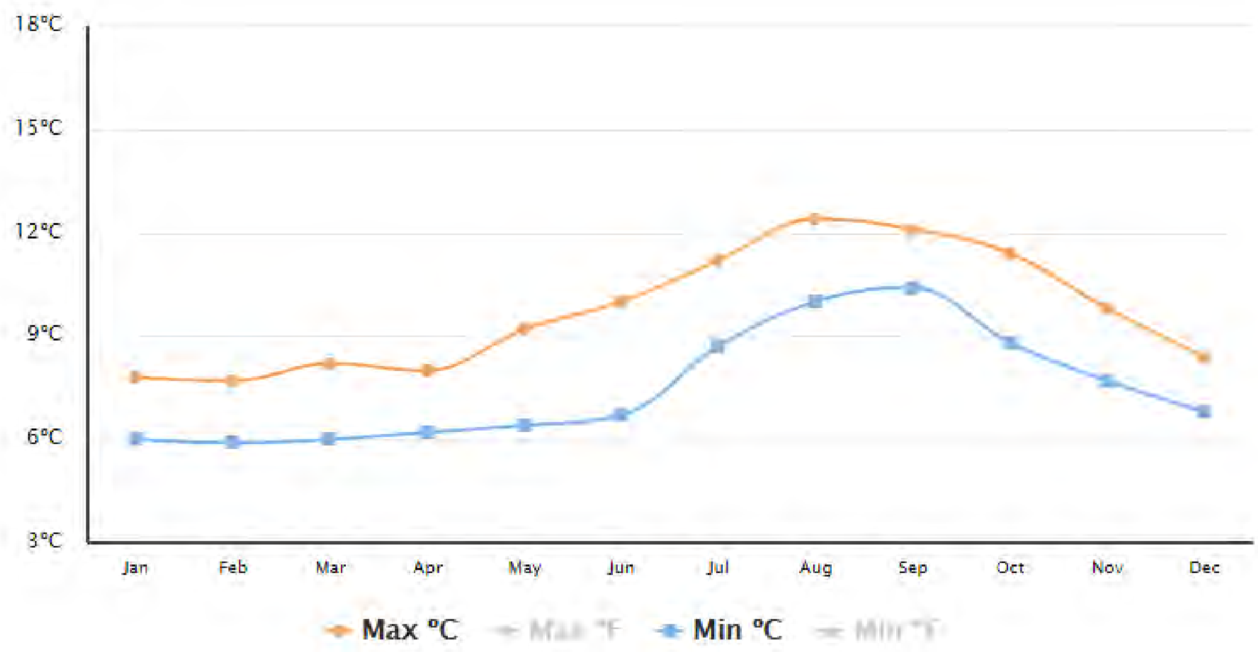

Figure 3.4: Average Sea Temperatures for Vancouver, Canada [27]

Then, using the relationship for Reynold's number,

$$Re = \frac{vl}{\nu} \qquad \text{[Eqn. 4]}$$

where, Re is the Reynold's number, l is the chord length of the wing cross-section, and ν is the kinematic viscosity of the water, and v is the fluid velocity, the Reynold's number was found to approximately 7.99E+05. This was calculated by averaging four values of Reynold's numbers across the expected operational velocity range identified during the design review of the surf foil (5, 6, 7, and 9 m/s).

The results are tabulated in Table 3.2.

Table 3.2: Reynold's Number Calculations for Lift, Low Range, Mid-Range, and Maximum Velocities.

Re lift	Re low	Re Mid.	Re max.	T [°C]	Kin. Viscosity [m^2/s]
4.62E+05	5.55E+05	6.47E+05	8.32E+05	2	1.6736E-06
4.93E+05	5.92E+05	6.91E+05	8.88E+05	4	1.5674E-06
5.26E+05	6.31E+05	7.36E+05	9.46E+05	6	1.4716E-06
5.58E+05	6.70E+05	7.82E+05	1.01E+06	8	1.3849E-06
5.92E+05	7.11E+05	8.29E+05	1.07E+06	10	1.3063E-06
6.26E+05	7.52E+05	8.77E+05	1.13E+06	12	1.2347E-06
6.62E+05	7.94E+05	9.26E+05	1.19E+06	14	1.1692E-06
6.97E+05	8.37E+05	9.76E+05	1.26E+06	16	1.1092E-06

NOTE: The values are calculated for a range of water temperatures.

After running the XFOIL simulation several iterations using varying angles of attack, the team was able to gain valuable insight into the expected behaviour of the chosen NACA 23015 profile. The graphical and vector representations of the pressure distribution gave the team insight into the location of the centre of pressure, which was a consideration during the design process, particularly in determining the ideal mounting hole locations on the wings. The team opted to place the mounting holes in the region where the centre of pressure would primarily act (note that the centre of pressure location changes with varying conditions) in order to minimize the bending moment induced on the wing.

An anhedral shape was selected to increase the maneuverability of the front wing. The curve of the anhedral shape is based on a Bezier curve, which is a practical and visually pleasing arc [28]. The rear wing provides stability to the system, as a result the wing is flat to assist with pitch stability. The chord length selected is a result of the required surface area to generate lift at the lower operational foiling velocity while maintaining a structurally sound core that assists with the ease of manufacturing.

Both front and rear wings are quasi-elliptical in shape, which increases the overall surface area.

The chord length varies throughout the span of the front wing. The rear wing chord length remains constant for most of the wingspan and only tapers close to the tips.

3.1.1.1 Parametric SolidWorks® Wing Models

The Airfoil Tools website was an excellent resource that provided detailed information on the shape and properties of a wide variety of NACA profiles. The NACA 23015 profile was selected for the surf foil [25]. The website generates a 2D cloud in a text file. Using the "Code for Processing NACA Profiles into SolidWorks® Readable File" [Appendix D], the data file was converted into a 3D point cloud that can be imported to SolidWorks®.

Once the 3D point cloud was imported, the offset function with zero offset selected was used to connect the points together. Construction geometry was added to the sketch to assist with constraining the profile. It is recommended to add a straight line from tip to tail and points at one quarter marks along its length for reference later. The offset sketch was converted into a block. The wing profile block was easier to manipulate and scale than the offset sketch and the block can be easily placed where needed in the model. The block referred to here is shown in Figure 3.5.

Figure 3.5: NACA 23015 SolidWorks® Block

The wing profile block was constrained to the center of the part file so that only one half of the model needed to be drawn, the remaining half was mirrored. Planes offset from the origin by know distances were used to allow for easy modifications to the span and provided a convenient element to constrain the blocks to, they are shown in Figure 3.6. Planes were created in the front and top orientation at the desired distances. Blocks were imported and constrained to these points, the front wing model was sectioned into three parts

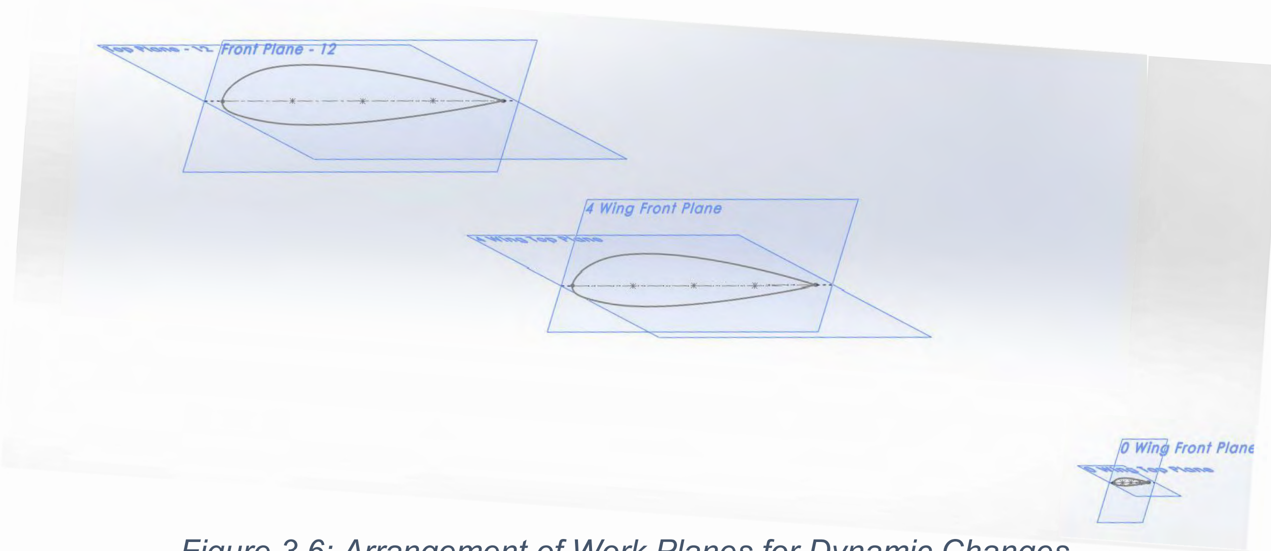

Figure 3.6: Arrangement of Work Planes for Dynamic Changes

The loft feature was used to generate much of the wing. To generate the elliptical shape along the wing, a 3D sketch with the Style Spline/Bezier tool was selected. The loft feature was used to connect the two blocks at both ends of the 3D guide sketch. The "To Next Sharp" option was used to provide a solid trailing edge. The mirror feature was used to create the other side of the wing.

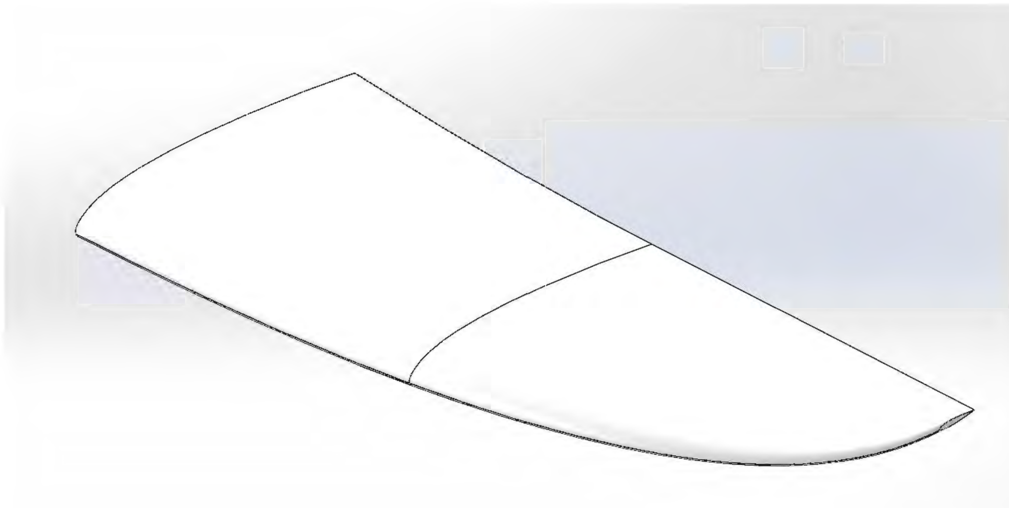

Figure 3.7: Modeled Front Wing in Sections

The fuselage interface is tangent to the highest point on the NACA profile, which is located at the first quadrant of the image in Figure 3.7. The interface is parallel to the initial top plane of the model, which places the wing at a neutral attack angle. A sketch was created at the origin and extruded in both directions to create the interface and the ramp. A 45° chamfer was then created on the side of the interface to create the lateral ramps.

The holes for the M8 fasteners, shown in Figure 3.8, were located towards the center of the wing, and 2" apart from center to center. The standard hole-wizard tool could not be employed as the resulting shape did not allow for the fastener heads to sit flush to the wing. The through holes were created at 0.354in in diameter to allow a tight tolerance without interference. The M8 fasteners have a 90° countersink, which was achieved by sketching a 45° triangle aligned with the highest tangent point of contact with the wing and modeled using the revolve tool.

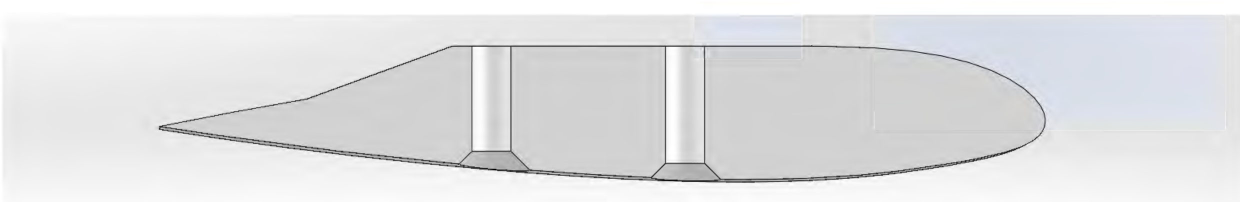

Figure 3.8: Fuselage Attachment Cross-Section

To create the STL files required for 3D printing, planes are created at each interface. The wing must be cut into several pieces for 3D printing due to the limited bed space. To assist with assembly, ¼" holes were modeled mid plane where the segments interface so that dowels could join the parts. These holes are shown in Figure 3.9. The Configuration Manager in SolidWorks® is used to generate a configuration for each segment. Each configuration can be saved as an individual STL file using the "Save As" tool and selecting the correct extension.

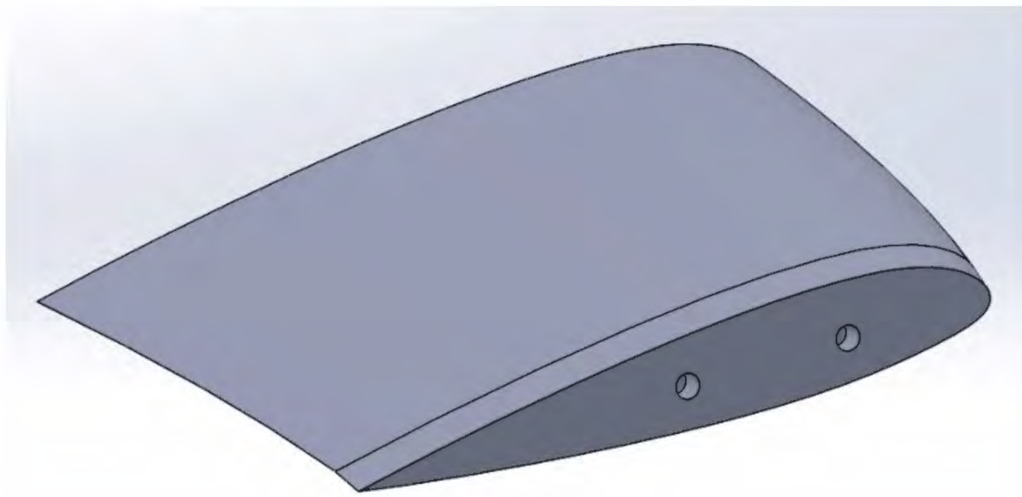

Figure 3.9: Mid-Section of Front Wing for 3D Printing

The carbon fibre texture used in the assembly, is shown in Figure 3.10, and can be found under the carbon fibre aramid fabric. The resulting models closely resembled the finished product.

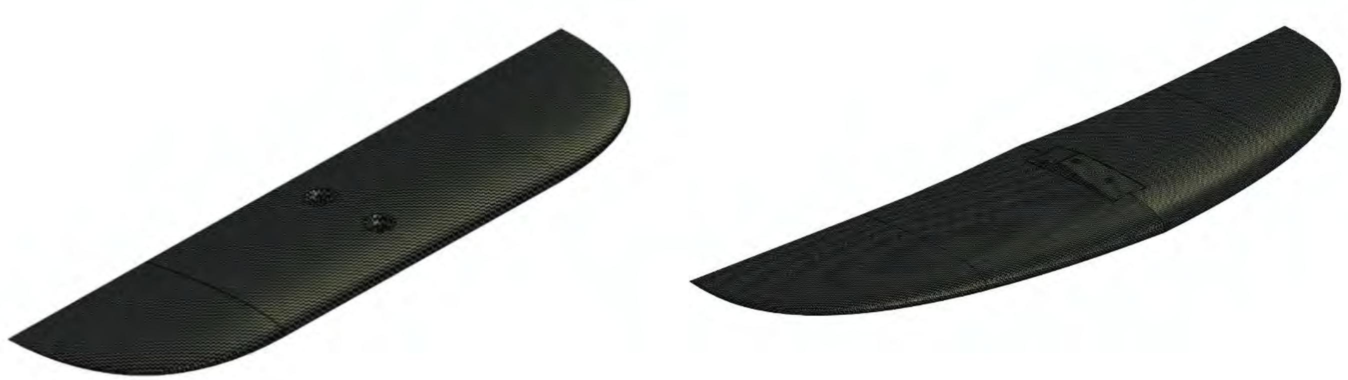

Figure 3.10: Final models Left: Rear wing, Right: Front wing

3.1.1.2 Crush Protection on Wing Attachment Points

A major concern for the design team, which was also mentioned during the critical design review is the ability of the PLA core of the wings to withstand the applied forced through the mechanical fasteners. To provide greater strength in the area, the wall thickness of the center core of the wings were printed with 3.2mm in order to create a more solid block of PLA. The yield strength of the PLA in the core cannot be taken as if it were created from an injection molding machine as the additive manufacturing process does not generate isentropic material structure.

The full calculations for the maximum allowable force can be found in Appendix E.

The assumptions and results of these calculations are: The estimated core yield strength of the 3D printed PLA is 3.77ksi [29]. Measurements for the bolts were taken from the supplier [30]. The contact surface area is 0.465in^2 and the max allowable force is 1760lb. This results in a safety factor of nearly six when comparing to the lifting force at 11mph.

3.1.2 Fuselage Design

A Cabrinha fuselage made available for examination and reverse engineering. The Cabrinha fuselage was 24 inches in length with a rounded top, flat base, machined grooves along each side, and a blue anodized finish. The front and rear wings both mounted to the flat underside of the fuselage, while the mast was mounted to the top by way of a milled cut-out of the mast profile. All fasteners for this fuselage were M8x1.25mm stainless steel countersunk screws.

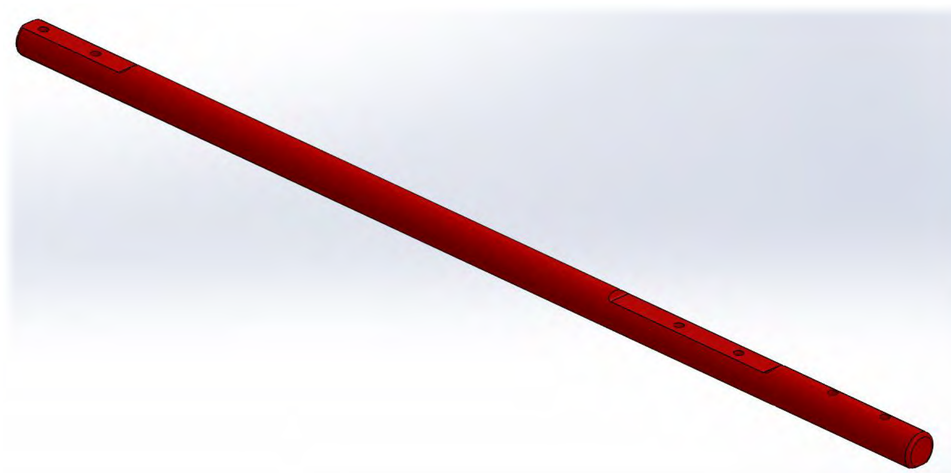

Figure 3.11: Fuselage design in SolidWorks®

The fuselage for this project was designed to be machined from one-inch round-stock aluminum, as shown in Figure 3.11. The loading expected for the fuselage is detailed in Appendix F "Fuselage Length Calculations".

In order to control the pitch angle while surfing, the rider shifts their weight or footing either forwards or backwards. This increases or decreases the distance between their center of gravity and the mast. This value is shown as the distance d in Appendix F. At lift velocity, the lift forces of the front and rear wings were calculated to be 294lb and -78lb, respectively.

To solve for the distance between the mast and the front end of the fuselage it is assumed that the length of fuselage between where the two wing forces acted is 26.5 inches and that the rider balances the board by shifting their center of gravity forward by 15.25 inches. From these assumptions, it was calculated that the fuselage should be centered on a point 4.604 inches from the leading edge of the fuselage.

Figure 3.12: Initial Fuselage Design - Side View.

The initial design, shown in Figure 3.12, had two opposing faces milled into the round-stock along the entire length of the fuselage. The cuts were 0.125 inches deep, leaving 0.75 inches of material in the fuselage.

The second iteration of the fuselage design had three milled cuts in the extruded round-stock, two on top and one on the bottom, these serve as an even interface for the attachment points of the front and rear wings as well as the mast. The mast attachment holes were designed to be through holes with a diameter of 0.345 inches, which ensures a tight tolerance with the M8 fasteners. The four holes for front and rear wing attachment were modeled to be the tap drill diameter for an M8x1.25mm fastener, 17/64 in. The resulting shop drawing for the fuselage is shown in Appendix G "Fuselage As-Built Shop Drawing".

The front wing was designed to generate lift upwards, so the fuselage was designed to have the front wing mount from the bottom with two M8x1.25mm fasteners threaded through the wing and into the fuselage. This will load the front wing in compression, which is desirable due to the PLA wing core. The rear wing mounts to the top side of the wing because it was designed to generate a downforce, which again puts the wing loading in compression. Fillets were applied to the milled-out cuts to smooth out the transition between the milled face and the original profile and reduce stress concentration points. The side view of the fuselage, shown in Figure 3.13, displays these features and notes the location of the other components.

Figure 3.13: Fuselage As-Built - Side View

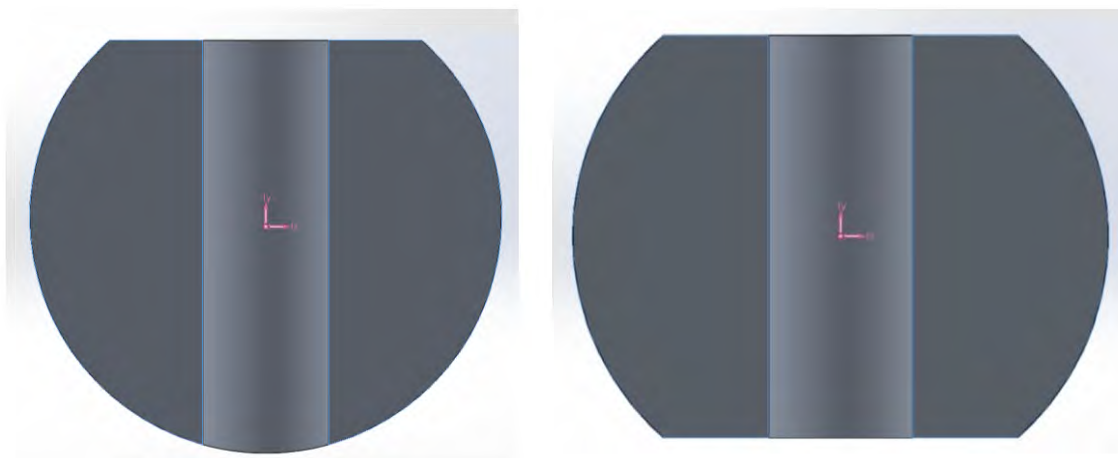

Figure 3.14:9 (L): Cross-Section - As-Built Fuselage, (R): Cross-Section - Initial Fuselage Design

The loading from the wings on the fuselage described above was used to perform bending stress calculations. These calculations are shown in Appendix H “Fuselage Stress Calculations”. Figure 3.14 shows the original fuselage design as well as the as-built fuselage. The moment of inertia for the original fuselage design was found to be 0.019133 in^4 and 0.023085 in^4 for the as-built design. These values were used in calculating the expected bending stress using the formula:

$$\sigma_{max} = \frac{Mc}{I} \qquad \text{[Eqn. 5]}$$

As was the assumed maximum bending moment of 208 Nm (135 ft.lb) which is shown in the related appendix.

The maximum bending stress in the original design was calculated as 249 MPa (36 ksi) and 206 MPa (30 ksi) for the as-built design. Given that the yield strength of 6061 aluminum is 276 MPa (40 ksi) both fuselage designs would be safe.

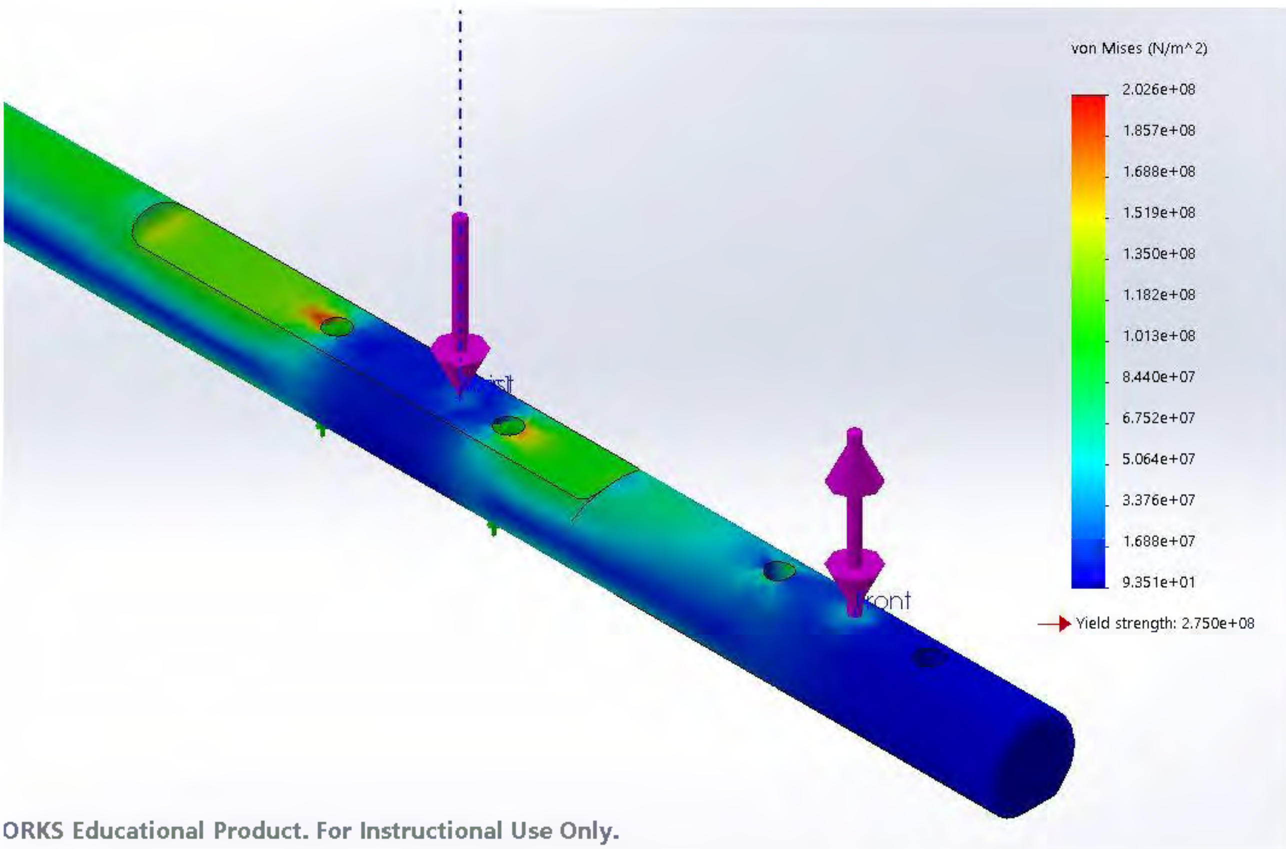

Figure 3.15: SolidWorks® Finite Element Analysis Output for Fuselage

The hand calculations were verified with SolidWorks® finite element analysis (FEA), shown above in Figure 3.15. One possible reason for the difference in stresses between the hand calculations and the SolidWorks® FEA is that the fuselage was fixtured by the bolt holes for the mast connection to the fuselage in SolidWorks®, whereas the hand calculations assumed a point fixture located 4.604 inches from the front of the fuselage. However, the two methods yielded similar results, 202 MPa (29.3 ksi) from SolidWorks® compared to 206 MPa (29.9 ksi) by the hand calculations.

3.1.3 Mast Design

Two commercially available masts were examined, a Cabrinha and a Slingshot, both of which resembled symmetrical NACA profiles. Reverse engineering through careful measurement revealed that the Cabrinha mast used a NACA 0012 profile.

The mast was designed with the symmetrical NACA 0012 airfoil. Like the process detailed above for the wings, the NACA profile was transferred to a SolidWorks® readable format using the "Code for Processing NACA Profiles into SolidWorks Readable File" [Appendix D]. A block was created from the curve so that its overall size could be scaled as needed without distorting the profile. The mast profile was then extruded to five inches which will accommodate the print volume of most additive manufacturing devices.

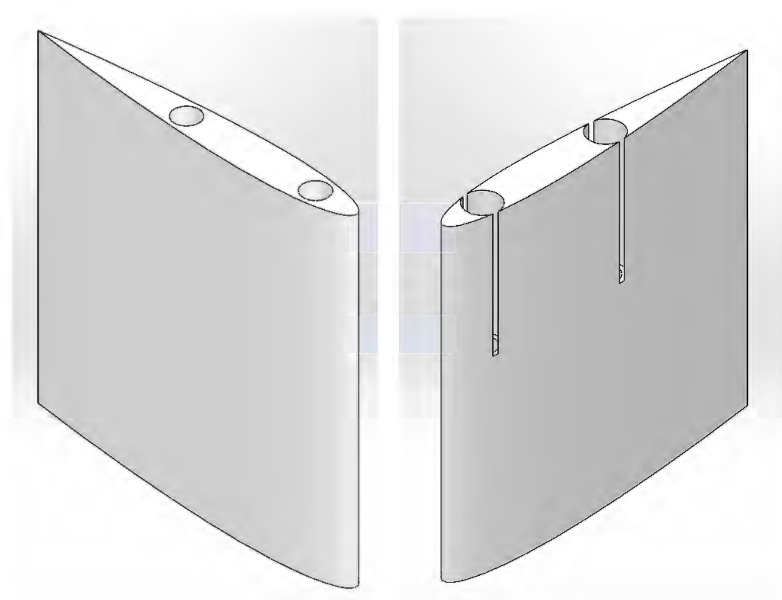

Figure 3.16: Midsection & End Section of Mast Profiles

For 3D printing the mast needed to be split into end sections and midsections, shown in Figure 3.16. The midsections had a pair of extruded 0.375 inch diameter cylinders cut from them spaced two inches apart. The end portions of the mast required an additional cylindrical cut of 0.5 inches diameter by 2 inches deep in order to locate 0.5 inch round-stock that was drilled and tapped for M8x1.25 threads. The cylindrical cuts were modeled so that aluminum round-stock could be embedded into the 3D printed mast "sheath". The rods were not intended to be welded together, rather joined by epoxy to the PLA sheath and to each other.

Figure 3.17: Fully Assembled Mast Profile with Carbon Fibre Skin

The model was designed to take on the appearance of carbon fibre to resemble the intended finished product, as is shown in Figure 3.17.

3.2 Manufacturing Process

3.2.1 Front and Rear Wing Manufacturing

The competed SolidWorks® models of the front and rear wings were cut into sections along their cross-sections in order to accommodate a 3D printer with a standard print volume of 220x220x220 [mm^3] (8.66x8.66x8.66 [in^3]). In preparation of joining the wings, a hole and dowel system was devised at each section cut, such that the wings could be joined using epoxy after printing was completed. Below in Figure 3.18, the hole and dowel system for locating the adjacent part is shown on a section of the front wing.

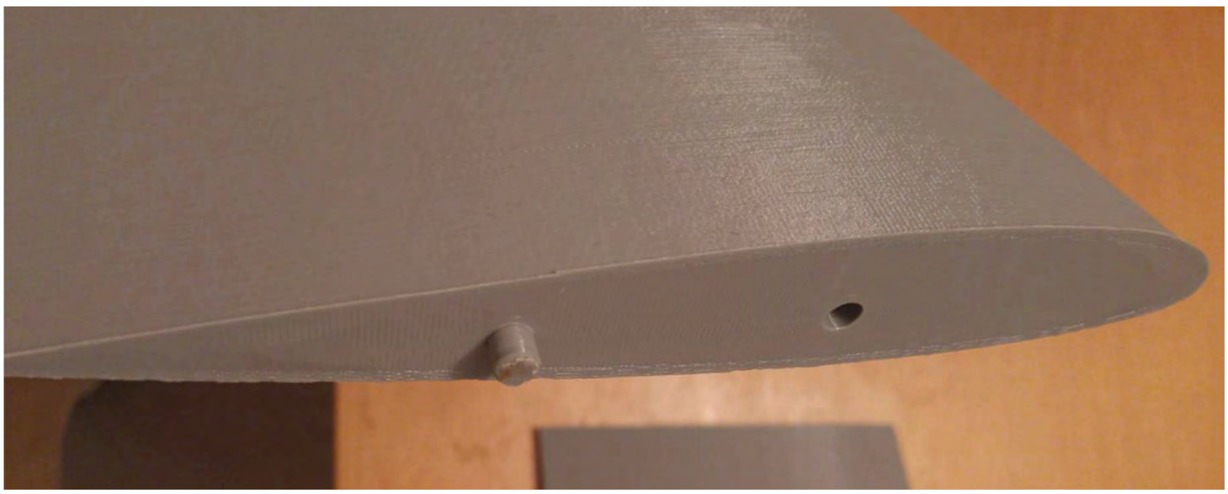

Figure 3.18: Hole & Dowel System used for Joining Wing Sections

3.2.1.1 3D Printing – Additive Manufacturing

Due to the complex wing geometry, 3D printing was well-suited to achieve the desired shape of the wing cores. As mentioned above, the wings were separated into sections and printed vertically in order to accommodate the 3D printer's printing capability and provide the highest quality print without the use of support material. Several preliminary wing designs were able to be printed so that they could be evaluated further. This method of rapid prototyping proved to be an invaluable tool during design review as it allowed the team to anticipate several issues that arose prior to carbon fibre layup. Below in Figure 3.19, a wing section is shown during printing.

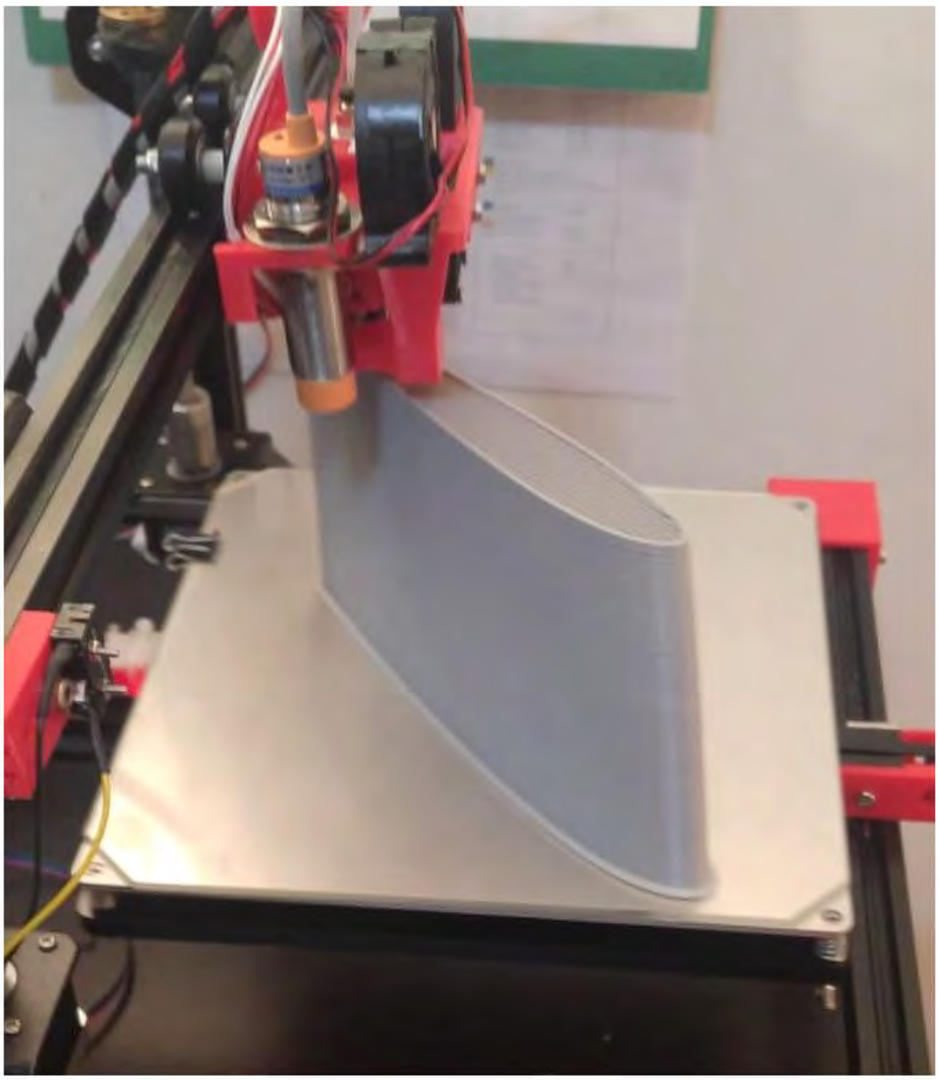

Figure 3.19: 3D Printing Front Wing Section

3.2.1.2 Wing joining and layup preparation

The wing sections were connected with the designed dowel-pin system and epoxied together using JB Weld KwikWood® epoxy. The epoxy at the joints was sanded down flush with the surface of the wing to prevent visual defects in the finished product. The 3D printing resulted in a rough surface due to the filament layer height, this was smoothed out by applying drywall putty and sanding. The wing shown in Figure 3.20 has had the epoxy and drywall putty applied. The wings were then painted using grey spray on primer and allowed to dry.

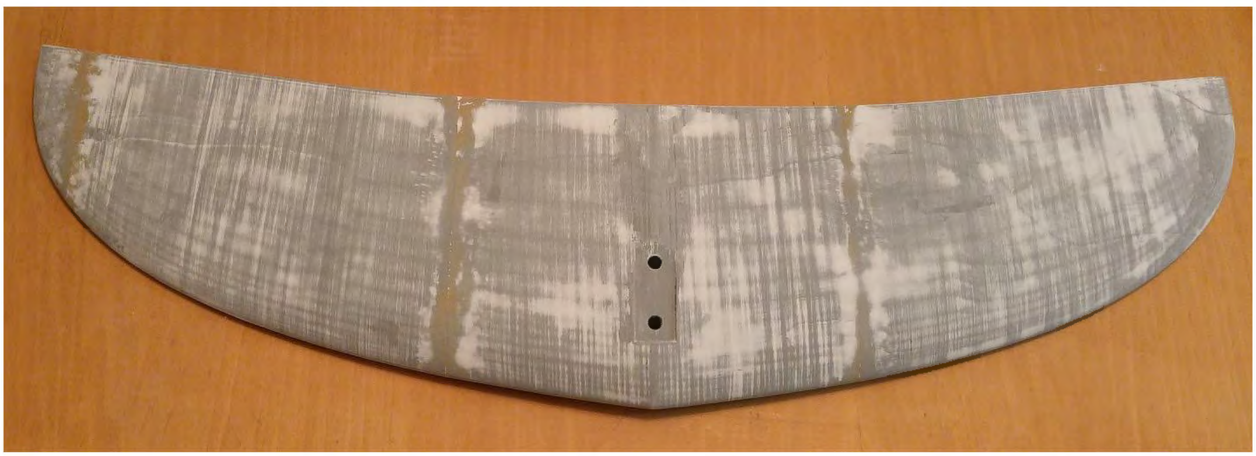

Figure 3.20: Prototype Wing Epoxied Together, Drywall Putty Applied, & Sanded

3.2.1.3 Carbon Fibre and Epoxy Layup

Woven carbon fibre sheets were cut to fit over the wing, with fibres oriented on 0^o-90^o and 45^o-135^o to ensure quasi-isotropic properties were achieved for the laminate. This fibre architecture is well suited to take the complex loading that will be applied to the wings. The epoxy used was "Cold Cure" by System Three, it has a cure time of approximately 35 minutes, and worked suitably as a top coat when applied thinly to the wings after layup and curing.

Figure 3.21: Application of Epoxy to the Front Wing Prototype

The wings were brushed with epoxy prior to the application of the first layer of carbon fibre, as shown in Figure 3.21. This was done to ensure good adhesion of the carbon fibre to the PLA core.

Figure 3.22: Application of the First Carbon Fiber Layer to the Epoxied Wing Core

The first layer of carbon fibre was then applied to the wing, careful consideration was given to ensuring the fibre weave conformed to the leading-edge geometry of the wing. This process is shown above in Figure 3.22.

For the prototype wing the carbon fibre was made to conform to the leading edge of the wing up to approximately 3 inches from the wingtips, after which darts (i.e. relief cuts) were cut into the carbon fibre and it was folded back onto itself. This method proved to be problematic as it required a considerable amount of skill to execute well. Furthermore, it resulted in loose fibre strands adhering to the outside surface, which appeared as visual artifacts on the finished product.

For the second prototype of the front wing, the carbon fibre was made to conform to the wing up to approximately 3 inches from the wing tip and then was allowed to naturally run out from there. When the epoxy cured this excess flashing was cut off using a pneumatic die-grinder.

Figure 3.23: Application of the Second Carbon Fibre Layer.

The surface of the first layer of carbon fibre was painted with epoxy, then the second layer of carbon fibre was applied, as shown in Figure 3.23. The second layer of carbon fibre was oriented 45^{o} to the first layer. With the two layers of carbon fibre applied, the wing was wrapped in peel-ply, a thin white fabric that ensures an even surface finish and easy removal of material after the epoxy has cured. This was followed by a breather cloth, a fluffy, low density material that allows air to be removed from the vacuum bag. The wing, wrapped in breather cloth, was placed inside a clear plastic sheet and sealed with two-way adhesive with a hose penetrating one edge and touching the breather cloth as shown below in Figure 3.24. A vacuum pump removed excess air for several hours while the epoxy cured.

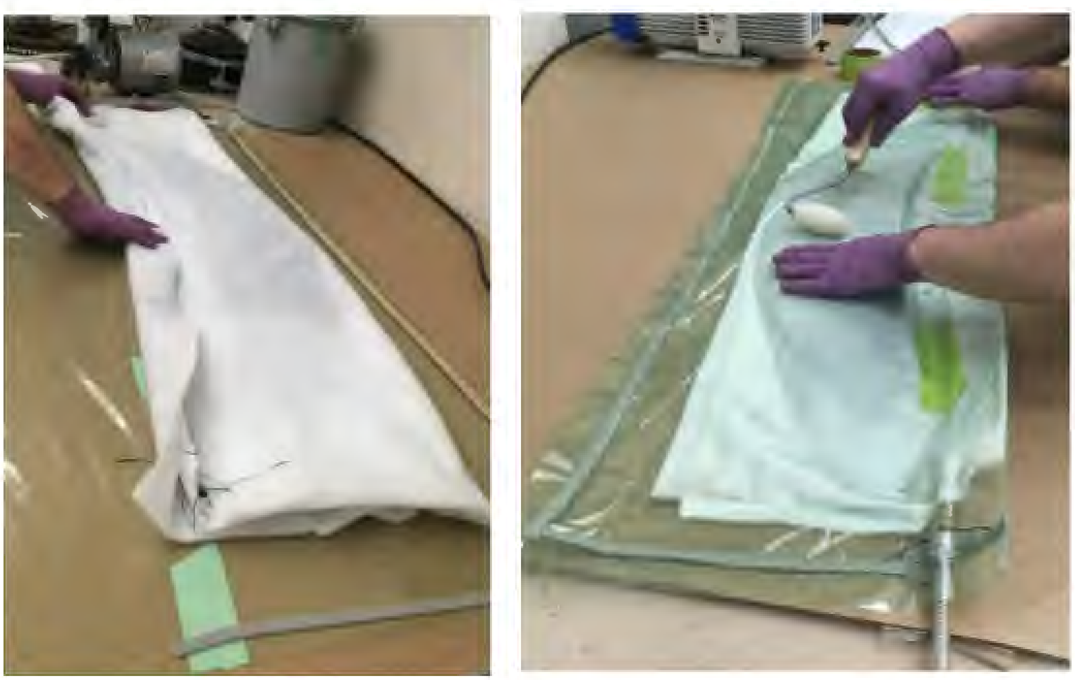

Figure 3.24: (L) Wing Wrapped in Breather Cloth (R): Wing sealed in the vacuum bag.

3.2.1.4 Wing Finishing

To achieve a glossy clear finish, two additional layers of Cold Cure epoxy were applied to the surface of the wings.

After the wings were removed from the vacuum bag process detailed in the previous sections, a thin coat of epoxy was applied to the top and bottom surfaces. These applications were done one surface at a time (i.e. top of the wing, then bottom of the wing) and allowed to cure before moving on to the other surface. This prevented drips from forming, which had occurred on the first prototype when it was hung to dry.

The first topcoat of epoxy was then sanded with successively finer grits of sandpaper, from 220 to 1500 grit (220, 400, 600, 1500), to even out the surface. Careful attention was paid to not sand through the carbon fiber and epoxy, especially at the wingtips, which had occurred on the first prototype.

A second coat of epoxy was applied, again thinly, according to the same procedure as the first application. The second layer of topcoat epoxy was also sanded with 220 to 1500 grit sandpaper. The resulting surface was smooth to the touch and the carbon fiber was clearly visible through the topcoats.

Several coats of Rust-Oleum® Painters Touch Ultra Cover Clear Gloss spray on clear coat were applied to the wings. The advantage of this is that it provides UV protection to the epoxy and it provides a “wetted” surface to the wings. The resulting finish was striking, the carbon fiber showed through well and caught the light. This is shown in Figure 3.25 below.

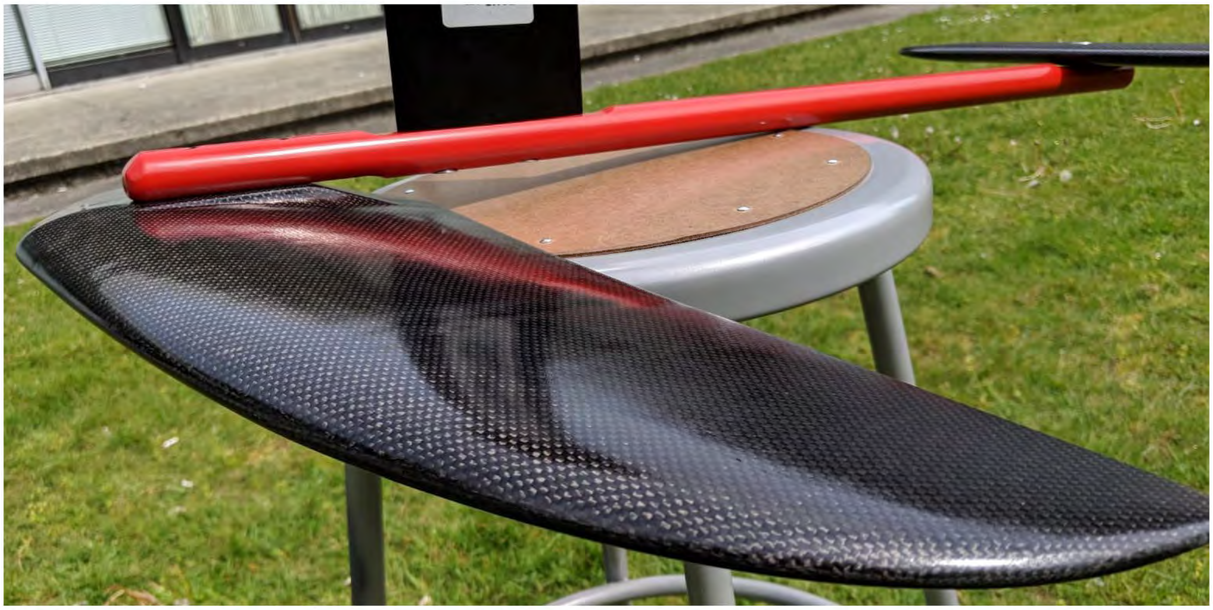

Figure 3.25: Front wing with clear coat and top coat applied.

3.2.2 Fuselage

The fuselage was manufactured according to the shop drawing shown in Appendix G "Fuselage As-Built Shop Drawing". The design of the fuselage was detailed Section 3.1.2.

A 30-inch section of one-inch diameter round-stock aluminum was cut using a descending bandsaw. The section of aluminum was fixed in two parallel vices on the bed of a milling machine, shown below in Figure 3.26. The milling machine ensure accurate machining due to the high tolerances of the digital controls.

Figure 3.26: Aluminum Fuselage Fixed in Vices on Milling Machine

Figure 3.27: Edge Finder Used on Fuselage

The rough-cut ends of the fuselage were trued using a ¾ x ¾ three flute end mill. An edge finder was used to locate the faces of the fuselage and zero the coordinates of the milling machine, this is shown above in Figure 3.27. Material was removed 0.020 inches at a time to a depth of 0.125 inches where required.

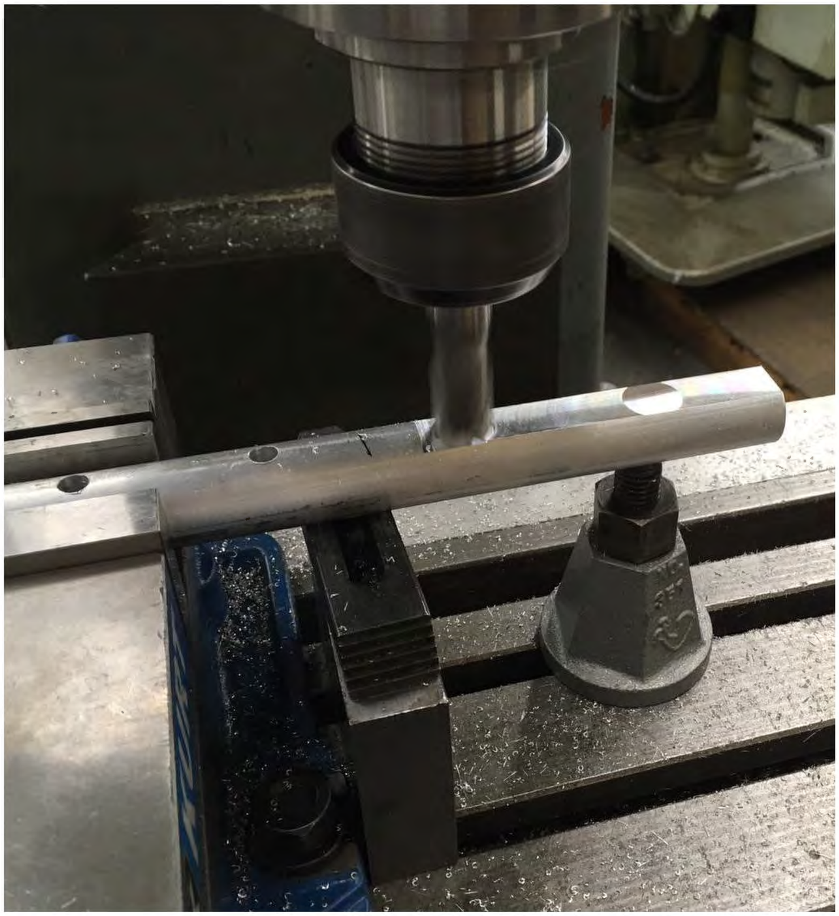

Figure 3.28: End Mill Removing Material from Fuselage

A ¾ x ¾ three flute end mill was used to make the 0.125-inch-deep cuts for the wing and mast interfaces through successive passes removing 0.020 inches of material with each pass. This process is depicted above in Figure 3.28. The rear wing and mast interface cuts were made on the top side of the fuselage, per the shop drawing. The required holes were drilled using the milling machine, pilot holes were drilled with a 1/8-inch drill bit for locating all holes. The mast connection holes were drilled out using an 8mm drill bit to allow the fasteners to freely pass through to the threaded connections in the mast. For the rear wing attachment holes a 17/64-inch drill bit was used, which is the required tap drill size for a M8x1.25mm tap.

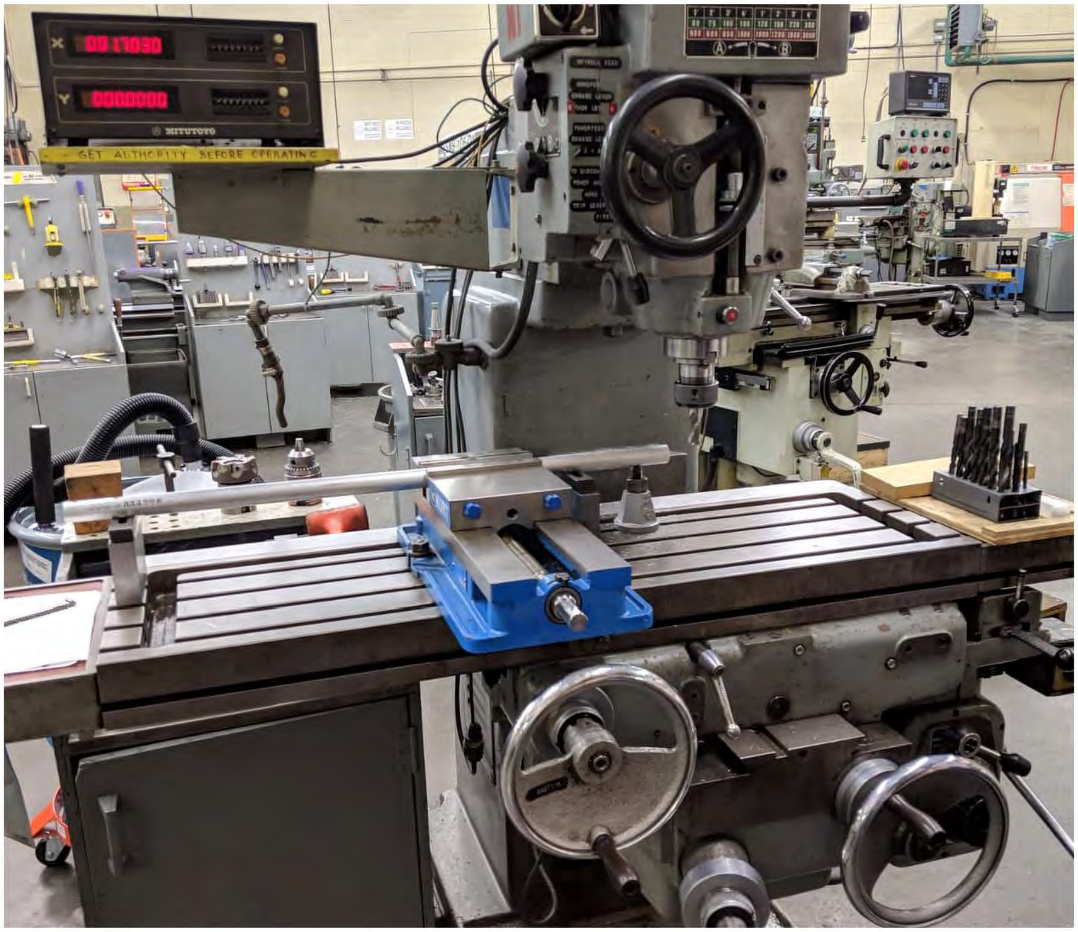

Figure 3.29: Fuselage Prior to Machining Front Wing Interface

The fuselage was rotated 180^{o} and the two milled cuts were supported with two machined blocks of equal height to ensure that the fuselage was parallel to the milling bed and did not deflect away from the bit during machining, this is shown above in Figure 3.29. The edge finder was used to zero the milling machine. With the fuselage rotated the bottom side of the mast attachment holes were chamfered to fit the countersink screw heads. The milling passes for the front wing attachment were made in the same fashion as for the rear wing and mast. The method of drilling the front wing attachment holes was the same as the rear wing holes detailed previously.

Figure 3.30: Tapping Operation for Wing Attachment Holes

The wing attachment holes were tapped to M8x1.25mm threads using a hand turned tap. The fuselage was clamped in a bench vice for this operation, shown in Figure 3.30.

Figure 3.31: Fuselage with Rounded Profile & Sandblasted Finish

The stepped edges of the milling cuts, shown above in Figure 3.31, were radiused using a half-round file, this could also be achieved by using a different style of cutting head during the milling operation. The leading edge of the fuselage was rounded out using a file to the shape. All deep scratches were removed from the fuselage using a fine-toothed flat file. The fuselage was sandblasted to even out the surface finish prior to powder coating, the sand blasted fuselage is shown in Figure 3.31.

The fuselage was cleaned with isopropyl alcohol prior to ensure good adhesion between the aluminum fuselage and the raw powder coat particles. Red was the colour of choice because it is aesthetically pleasing and is not used by any popular commercially available manufacturers. The fuselage was hung in a powder application booth using a section of welding rod wrapped around a bolt threaded into the fuselage. Bolts were used to protect the threads from being powder coated as this would create undesired interference with the mounting fasteners. A large furnace was heated to 400°C and the coated fuselage was placed into the furnace for 20 minutes. After heating, the fuselage was removed and allowed to cool slowly. The results of this procedure are shown below in Figure 3.32.

Figure 3.32: Fuselage with Powder Coating

3.2.3 Mast

The mast designed for this project was not manufactured by the project team. The manufacture of this part will be completed shortly after the publication of this document by Chris Chambers of BCIT's TTED program.

The manufacturing process is similar to the process described for the wings, in that the core is manufactured, then wrapped in carbon fibre and epoxy composite. Sections of the mast are 3D printed out of PLA, epoxied together with two aluminum rods embedded into the mast. The embedded aluminum rods have their ends drilled and tapped to accept M8x1.25mm fasteners. The excess epoxy would be sanded down at the interfaces and then Bondo or drywall filler applied to the profile in order to even out the surface.

The mast would then be coated in epoxy and woven carbon fibre and vacuum bagged, following the same procedure detailed for the wings.

Figure 3.33: 3D printed mast core with aluminum connecting rods.

The pre-layup mast is shown in Figure 3.33 with the aluminum connecting rods epoxied in place.

4 Discussion of Results

4.1 Prototype Manufacturing Results

The result of the design and manufacture of a surf foil was successful. The surface quality of the carbon fibre wings is above expectation. Although they are not without some minor visual defects, they appear to be structurally sound and have passed an initial 3-point bend test. However, greater refinements to the efficiency of the manufacturing processes and the consistency of the finish is attainable. Such as finer resolution of prints and smaller prints through more segments.

The fuselage machining tolerances were well within the limits of variation and the overall fit of the attached parts is excellent. Initially an anodized finished was strongly considered, however; a powder-coating was selected as the process could be performed by the team inhouse.

A set of 3 masts were purchased from SlingShot®, as the team is planning on testing the product over the summer. The designed foil is being also constructed by Chris Chambers, a TTED student at BCIT, his will include the designed mast. Its completion will be after the publication of this report.

All external hardware such as the Slingshot® pedestal and FoilMount® surf foil mounting materials have been received. The purchase of the surfboard is still outstanding due to availability.

4.2 Project Management Results

The project management portion of the project was also successful. The preliminary documentation was completed on time and all major milestones were reached. The largest discrepancy with the Projected Gantt chart [Appendix I] and the actual time line was in the completion of the design and solid modeling work packages. It was initially projected to be completed January 14th but required an additional two months. This was due to the ease in which iterations of components can be created with additive manufacturing which led to a far more refined design.

The delay with completion of the solid modeling did not prevent the completion of the final product, which was right on schedule. The work remaining is a presentation to peers on the outcome of this project and a public exhibition of engineering capstone projects throughout BCIT.

5 Conclusion

5.1 Lessons Learned and Potential Improvements

The fuselage interface ramp angle is too steep for optimal forming of the carbon fibre and epoxy composite, particularly with respect to the front wing. This can be resolved by altering the model to prevent a pocket from forming at that junction or by building up on the core with a compound while the wings are being assembled.

In order to achieve a higher quality surface finish, it is imperative that the core is blemish free, as even small ridges will show clearly through the carbon fibre and epoxy composite treated with a clear finish. Surface imperfections are extremely difficult to improve, and the touch-ups may result in lower overall product quality due to excessive sanding of additional epoxy.

Prior to carbon fiber lay-up, the connections between wing segments need to be sanded flush to the wing surface. The final prototype has some minor blemishes as a result of these seams not being sufficiently sanded during the preparation phase.

Post layup, the wings should be protected from contaminants and handled with gloves. It is suspected that some of the minor surface imperfections in the finish are due to contaminants beneath the top coat of epoxy that were not removed by cleaning with isopropyl alcohol.

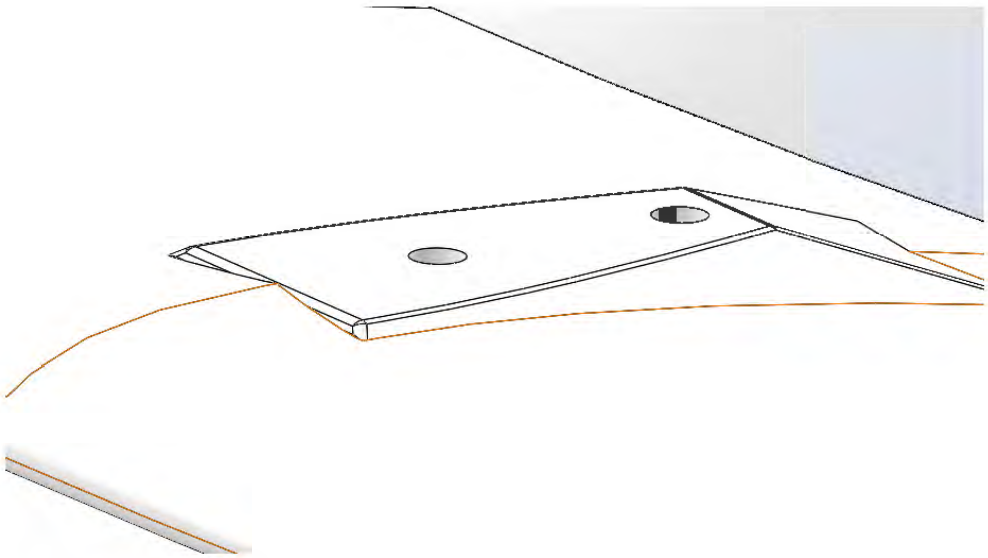

Figure 5.1: Fuselage Interface on Front Wing

The corner of the fuselage interface ramp, shown in Figure 5.1, sanded through very easily. This slowed the finishing process as additional care had to be taken in this area. This area should be redesigned so the front edge (left of center in Figure 5.1) is not proud of the wing surface and the trailing edge should be rounded out. Additional carbon fibre strips should be tested in this area to see if this prevents sand-through.

Clear coat should be applied on top of the sanded topcoats of epoxy to achieve a glossy clear finish that displays the carbon fiber pattern. When applying clear coat many light coats are best, as heavy applications of clear coat tend to run. Clear coat should be sprayed according to the instructions on the can.

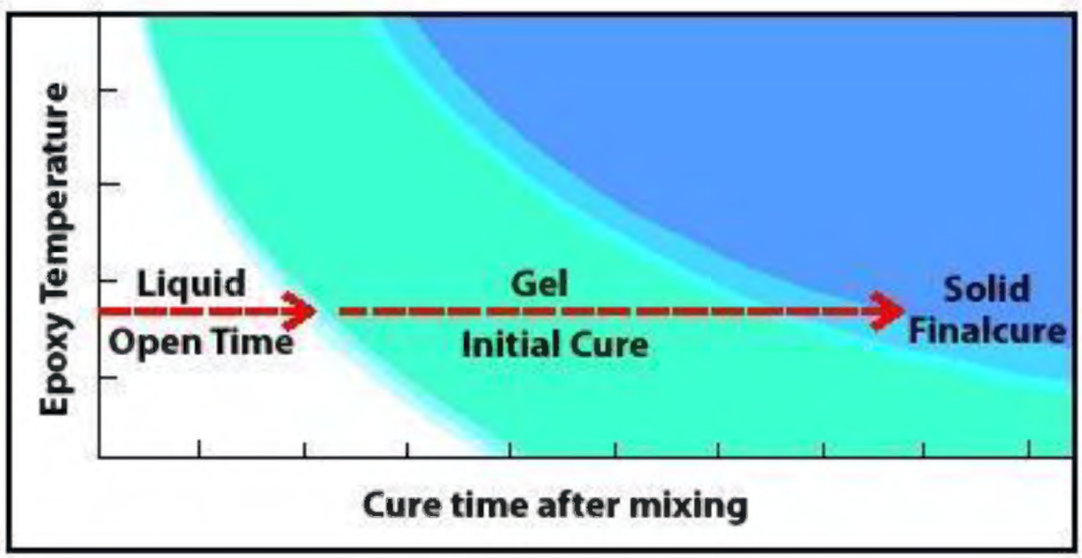

Figure 5.2: Plot of the relationship of epoxy cure time and temperature [31].

Epoxy cure time is closely related to temperature. Higher temperatures lead to faster curing, as shown in Figure 5.2.

Figure 5.3: Picture showing the circular region on the test wing.

When applying top coat epoxy to the first prototype wing plastic cups were used to support the wing while it was curing (epoxy had been applied to the opposite face of the wing). A circular region of epoxy with considerably better finish occurred on the area above where the cup had been placed. We theorize that the cup had captured some heat created by the exothermic curing of the epoxy and had sped up the cure of the epoxy in that area and the surrounding areas on the wing were pockmarked. This is shown in Figure 5.3.

As such, when applying the top coat of epoxy, the room temperature should be carefully controlled to ensure that the epoxy cures quickly to avoid spotty coverage. This is likely due to small scale high spots (<0.001 inches) that the epoxy flows away from to the surrounding areas.

5.2 Fulfillment of Project Objectives

The major objectives of the design and manufacture of a surf foil system were to create parametric 3D models of all the components, followed by their manufacture as well as full documentation of the progress of the project, including presentation to peers and the public.

Figure 5.4: Fully Assembled Surf Foil

All design objectives have been met. The manufacturing objectives have been met and the fully assembled surf foil is seen in Figure 5.4. The manufacture of the mast was not required because a set was purchased, and priority was given to the completion of project documentation and the exhibition of the project. The project is on schedule to meet the remaining documentation and presentation requirements.

All the information required to reproduce this product have been included with the hope that this work will aid in the development and advancement of surf foil technology.

6 Bibliography

[1] US Water Ski & Wake, "US Water Ski," 2013. [Online]. Available: http://www.usawaterski.org/pages/USA-WS%20Profile.htm. [Accessed 04 May 2019].

[2] S. Gill, "Is There an Average Weight for Men?," 14 February 2018. [Online]. Available: https://www.medicalnewstoday.com/articles/320917.php. [Accessed 04 May 2019].

[3] C. Muller, "Kite Hydrofoil," SABDA Studios, 2019. [Online]. Available: http://kitehydrofoil.com/index.html. [Accessed 02 March 2019].

[4] M. Todd, "How to Make Your Own Hydrofoil," Seabreeze, 2019. [Online]. Available: https://www.seabreeze.com.au/News/Kitesurfing/How-to-make-your-own-Hydrofoil_8649403.aspx. [Accessed 02 May 2019].

[5] Naish, "Thrust Windsurf Foil," Naish, 2019. [Online]. Available: https://www.naishfoils.com/product/thrust-windsurf-foil-complete-standard/. [Accessed 02 May 2019].

[6] SlingShot, "Aluminum Surf Foils vs. Carbon Surf Foils," SlingShot, 2019. [Online]. Available: https://blog.slingshotsports.com/aluminum-surf-foils-vs-carbon-surf-foils-which-is-better/. [Accessed 02 May 2019].

[7] IKO, "How to Choose your Hydrofoil Board," IKO, 2019. [Online]. Available: https://www.ikointl.com/how-to-choose-your-hydrofoil-board. [Accessed 02 May 2019].

[8] M. H. Sadraey, Aircraft Design: A Systems Engineering Approach, New Hampshire: A John Wiley & Sons, Ltd., Publication, 2013.

[9] A. Engineering, "Control and Stability of Aircraft," 23 January 2016. [Online]. Available: https://aerospaceengineeringblog.com/control-and-stability-of-aircraft/. [Accessed 04 May 2019].

[10] Warwickl, "Stabaliser Wing," Seabreeze, 03 June 2018. [Online]. Available: https://www.seabreeze.com.au/forums/Stand-Up-Paddle/Foiling/Stabaliser-wing-which-way-up?page=1. [Accessed 04 January 2019].

[11] C. Muller, "Design," SABDA Studios, [Online]. Available: http://kitehydrofoil.com/design.html. [Accessed 04 January 2019].

[12] C. Garbous, "Hydrofoil SUP - Kai Lenny's Board Explained," Total SUP, 04 May 2016. [Online]. Available: https://www.totalsup.com/news/kai-lennys-hydrofoil-sup-explained/. [Accessed 05 May 2019].

[13] Wikipedia, "Forward-Swept Wing," Wikipedia, 02 January 2019. [Online]. Available: https://en.wikipedia.org/wiki/Forward-swept_wing. [Accessed 04 January 2019].

[14] Wikipedia, "Delta Wing," Wikipedia, 09 December 2018. [Online]. Available: https://en.wikipedia.org/wiki/Delta_wing. [Accessed 04 January 2019].

[15] Wikipedia, "Wing Configuration," Wikipedia, 10 December 2018. [Online]. Available: https://en.wikipedia.org/wiki/Wing_configuration#Chord_variation_along_span. [Accessed 04 January 2019].

[16] D. F. W. Riefels, "Aerofoil Sections," Butterworths, London, 1961.

[17] T. V. B. C. W. a. R. R. G. Robert H. Neely, "Experimental & Calculated Characteristics of NACA 44-Series Wings," Langley Memorial Aeronautical Laboratory, Washington, 1947.

[18] Federal Aviation Administration, "Pilot’s Handbook of Aeronautical Knowledge," U.S. Department of Transportation, Oklahoma City, 2016.

[19] T. Benson, "Modern Lift Equation," NASA, 05 April 2018. [Online]. Available: https://wright.nasa.gov/airplane/lifteq.html. [Accessed 04 January 2019].

[20] Glen Research Center, "Shape Effects on Drag," NASA, 2019. [Online]. Available: https://www.grc.nasa.gov/www/k-12/airplane/shaped.html. [Accessed 05 May 2019].

[21] N. Hall, "The Drag Equation," NASA, 05 May 2015. [Online]. Available: https://www.grc.nasa.gov/www/k-12/airplane/drageq.html. [Accessed 04 January 2019].

[22] Foilever, "Technical Terms: Kitefoil and Windfoil," Foilever, 2017. [Online]. Available: http://www.foilever.com/en/content/11-technical-terms-kitefoil-windfoil. [Accessed 04 January 2019].

[23] J. Smith, "Kiteboarding," Power Kite Shop, [Online]. Available: https://powerkiteshop.com/kiteboarding/. [Accessed 05 05 2019].

[24] N. Hall, "Inclination Effects on Lift," National Aeronautics and Space Administration, 05 April 2018. [Online]. Available: https://www.grc.nasa.gov/www/k-12/airplane/incline.html. [Accessed 04 January 2019].

[25] Airfoil Tools, "NACA 23015," Airfoil Tools, 2019. [Online]. Available: http://airfoiltools.com/airfoil/details?airfoil=naca23015-il. [Accessed 03 May 2019].

[26] H. Y. Mark Drela, "XFOIL: Subsonic Airfoil Development System," 13 December 2013. [Online]. Available: https://web.mit.edu/drela/Public/web/xfoil/. [Accessed 3 November 2018].

[27] Wold Sea Temperature, NOAA, "Vancouver Sea Temperature," 2019. [Online]. Available: https://www.seatemperature.org/north-america/canada/vancouver.htm. [Accessed 04 May 2019].

[28] UNSW, "De Casteljau Bezier Curves and Design," University of New South Wales, 2019. [Online]. Available: https://www.futurelearn.com/courses/maths-linear-quadratic-relations/0/steps/12129. [Accessed 05 May 2019].

[29] S. Saunder, "Tensile Properties of 3D Printed PLA Specimens," 3DPrint.com, 16 January 2019. [Online]. Available: https://3dprint.com/233916/tensile-properties-of-3d-printed-pla/. [Accessed 05 May 2019].

[30] McMaster-Carr, "Metric 18-8 Stainless Steel Hex Drive Flat Head Screws," McMaster-Carr, 2019. [Online]. Available: https://www.mcmaster.com/countersunk-screws. [Accessed 04 May 2019].

[31] W. System, "Epoxy Chemistry," [Online]. Available: https://www.westsystem.com/instruction-2/epoxy-basics/epoxy-chemistry/. [Accessed 09 05 2019].

[32] R. H. Neely, "Experimental & Calculated Characterisics of NACA 44-Series Wings," Langley Memorial Aeronautical Laboratory, Washington, 1947.

[33] A. Udris, "What Are Canards?," BoldMethod, 14 July 2014. [Online]. Available: https://www.boldmethod.com/learn-to-fly/aircraft-systems/canards/. [Accessed 04 January 2019].

[34] N. Hall, "Airplane Parts and Function," NASA, 05 May 2015. [Online]. Available: https://www.grc.nasa.gov/www/k-12/airplane/airplane.html. [Accessed 04 January 2019].

[35] PB Kiteboarding, "Spotz Tuna 58cm 61cm Lightwind," PBK, 2018. [Online]. Available: https://www.pbkiteboarding.com/Kiteboarding-Snowkiting-Equipment/Spotz_Tuna_Hydrofoils_Kitefoils_Kiteboarding_Kitesurfing_Foils/Spotz_Tuna_Hydrofoils_Kitefoils_Kiteboarding_Kitesurfing_Foils.html. [Accessed 04 January 2019].

[36] RC Powers, "Anhedral Wings :: Detailed explanations of anhedral plane designs," RC Powers, 16 February 2009. [Online]. Available: https://www.rcpowers.com/community/threads/anhedral-wings-detailed-explanations-of-anhedral-plane-designs.234/. [Accessed 04 January 2019].

Appendix A: Original Request for Proposal (RFP)

Poseidon Adventures

Water Sports Equipment Manufacturing

Location: 123 Fake Street, Burnaby BC. V5G 4J3
Proposal Number: A001234
Date: October 16th 2018

Project Overview

Poseidon Adventures is a new company that is looking to manufacture high quality recreational hydrofoils in their Vancouver, B.C. location. The successful candidate will design, build and test a carbon fiber hydrofoil to be used recreationally with a wakeboard or wake-surf board. Poseidon Adventures wants a hydrofoil design that is based on a solid scientific foundation, rather than the industry prevalent process of trial-and-error.

Objectives:

The goal of this project is to develop and test a lightweight and durable composite hydrofoil for the recreational market. The hydrofoil should be designed for use with a wakeboard or wake-surf board and be tailored towards adult users in the North American market. The design must be competitive in terms of cost with similar high-end hydrofoils.

Successful execution of the project will be the development of a scientific approach to hydrofoil design. The design process must include applied aerodynamic wing theory to justify design choices. Specifically, with reference to the ways in which foil form, shape, and size affect the performance of the hydrofoil. After successful prototyping, Poseidon Adventures intends to produce 30 units per month of the designed hydrofoil at a high-quality level.

Scope of Project:

This Request for Proposal has been developed to secure design, manufacturing and testing services for the development of a recreational hydrofoil. The project must be fully executed before May 8th, 2019 in order to allow for beta testing during the summer recreation season. The deliverables of the recreational hydrofoil design project include, but are not limited to:

Design and Simulation Deliverables

Technical specifications
Concept design
Concept drawings
Detail design
Solid modeling

Figure A.1: Original RFP from Poseidon Adventures Ltd (p1/2).

Prototype Deliverables
Manufacturing drawings
Fully functional prototype
Technical manual outlining the manufacturing process

Product Testing/ Design Validation
Technical analysis
Design validation through testing

In addition to the above, the project team will take part in weekly meetings with the project sponsor to review progress. The project team will prepare an agenda prior to each meeting and will record meeting minutes.

Proposal Requirements
The proposal should be submitted in PDF form no later that 4:00 PM October 30th, 2018. Late submittals will not be considered.

Please note that all work must be completed by the recipient(s) of this RFP and sub-contracting of any project component must be approved by Poseidon Adventures. Include C.V.'s of all team members detailing relevant past work and an organizational flow chart detailing team members' responsibilities.

Regards,

C. Johnson

Cave Johnson

Poseidon Adventures CEO

604-555-1745

Figure A.2:Original RFP from Poseidon Adventures (p2/2).

Appendix B: Lift Calculations

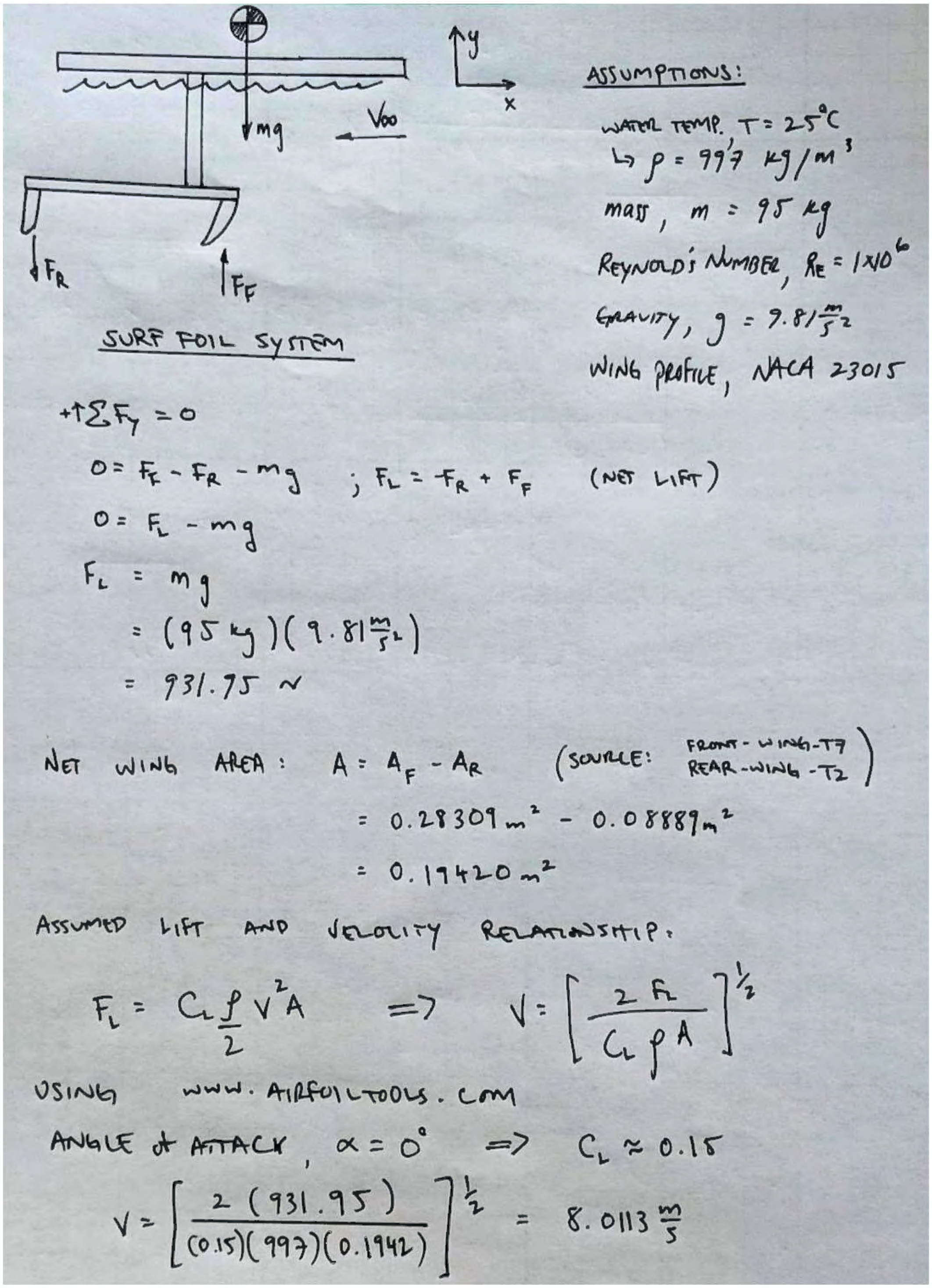

ASSUMPTIONS:

WATER TEMP, $T = 25°C$

↳ $\rho = 997 \ kg/m^3$

MASS, $m = 95 \ kg$

REYNOLD'S NUMBER, $R_E = 1 \times 10^6$

GRAVITY, $g = 9.81 \frac{m}{s^2}$

WING PROFILE, NACA 23015

$+\uparrow \sum F_y = 0$

$0 = F_F - F_R - mg \quad ; F_L = F_R + F_F$ (NET LIFT)

$0 = F_L - mg$

$F_L = mg$

$= (95 \ kg)(9.81 \frac{m}{s^2})$

$= 931.75 \ N$

NET WING AREA: $A = A_F - A_R$ (SOURCE: FRONT-WING-T7, REAR-WING-T2)

$= 0.28309 \ m^2 - 0.08889 \ m^2$

$= 0.19420 \ m^2$

ASSUMED LIFT AND VELOCITY RELATIONSHIP:

$$F_L = C_L \frac{\rho}{2} V^2 A \implies V = \left[\frac{2 F_L}{C_L \rho A} \right]^{1/2}$$

USING WWW.AIRFOILTOOLS.COM

ANGLE of ATTACK, $\alpha = 0° \implies C_L \approx 0.15$

$$V = \left[\frac{2(931.95)}{(0.15)(997)(0.1942)} \right]^{1/2} = 8.0113 \frac{m}{s}$$

Figure B.1: Minimum lift velocity calculations (p1/2).

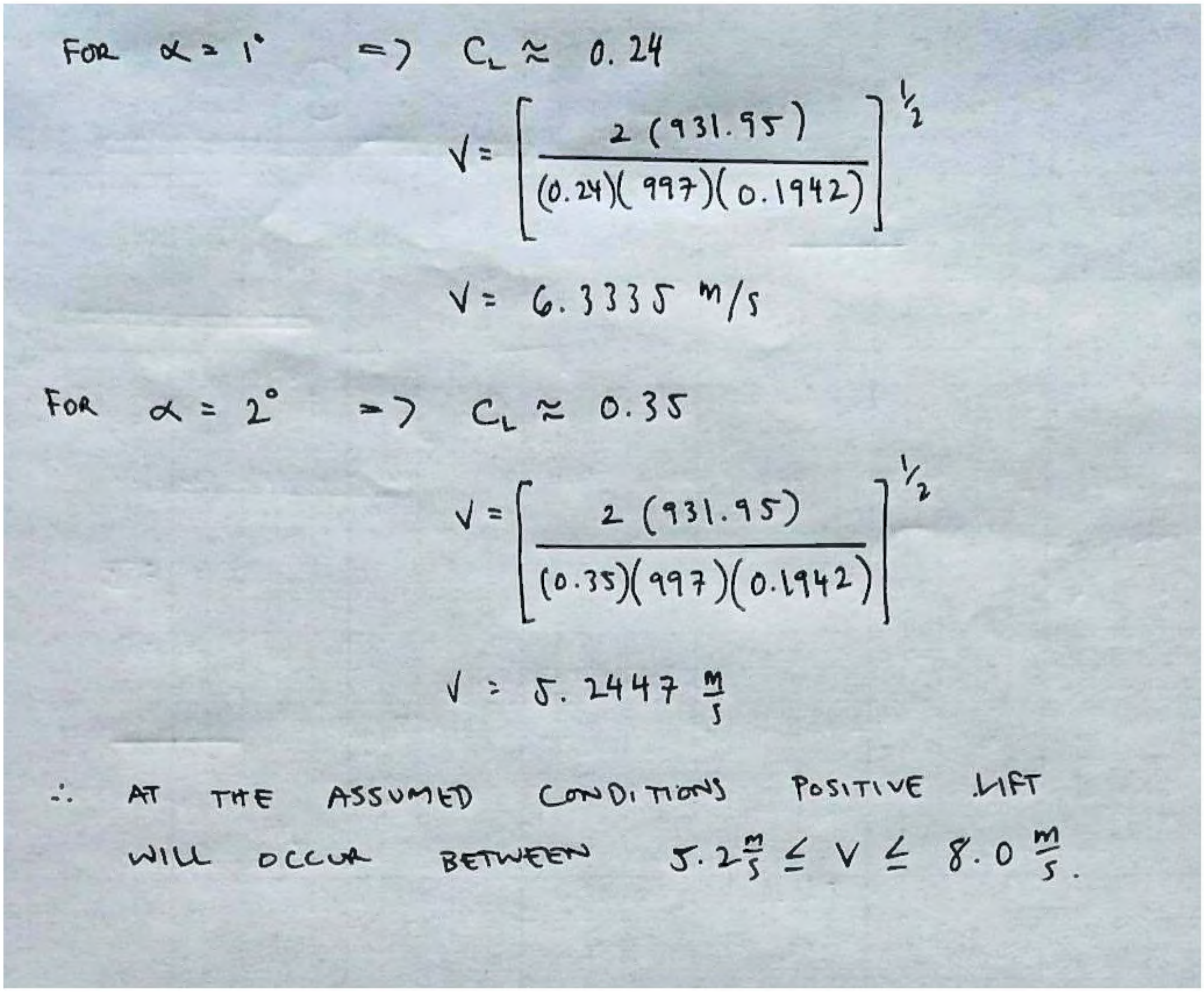

FOR $\alpha = 1^\circ \Rightarrow C_L \approx 0.24$

$$V = \left[\frac{2\,(931.95)}{(0.24)(997)(0.1942)}\right]^{1/2}$$

$$V = 6.3335 \ m/s$$

FOR $\alpha = 2^\circ \Rightarrow C_L \approx 0.35$

$$V = \left[\frac{2\,(931.95)}{(0.35)(997)(0.1942)}\right]^{1/2}$$

$$V = 5.2447 \ \frac{m}{s}$$

∴ AT THE ASSUMED CONDITIONS POSITIVE LIFT WILL OCCUR BETWEEN $5.2\frac{m}{s} \leq V \leq 8.0\frac{m}{s}$.

Figure B.2: Minimum lift velocity calculations (p2/2).

Appendix C: Design Review Package

Executive Summary

BTB Engineering will be conducting a critical design review on February 6th, 2019. The following document is provided to participants who are attending to inform them on the current state of the surf foil project as well as promote feedback in this stage of development.

The front and rear hydrofoil wings are NACA 23015 airfoil sections to be connected to a 1" diameter aluminum fuselage. The mast will have an aluminum core surrounded by a 3D printed form and covered with a carbon fiber skin. Assuming a combined board and rider mass of 95 kg the current design would have a "lift off" velocity of 11 mph.

The project is on schedule and on budget. BTB engineering will purchase the remaining components and materials at a total cost of \$1070 and commence manufacturing by February 13th, 2019.

Current Product Development Specifications

Design Load (Rider weight): 198 lbm (90kg)
Surf Foil Assembly Weight Target: 11 lbm (5kg)
Required Lift for Foiling: 209.5 lbf (932 N)
Minimum Foiling Velocity: 11.7 mph (18.8 km/h)
Maximum Foiling Velocity: 20 mph (32.2 km/h)

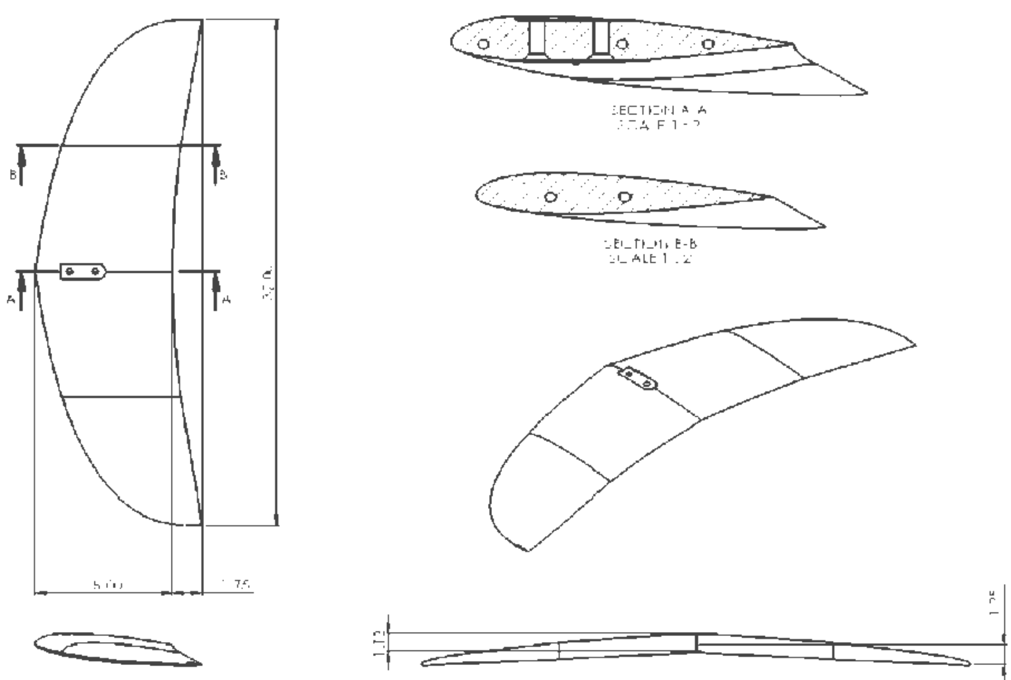

Figure 1: Drawing of current front wing design

Front Wing Span: 32" (813 mm)
Front Wing Chord Length: 8" (203 mm) - maximum
Front Wing Surface Area: 439in^2 (283090 mm^2)

Figure C.1: Design review package (p1/9).

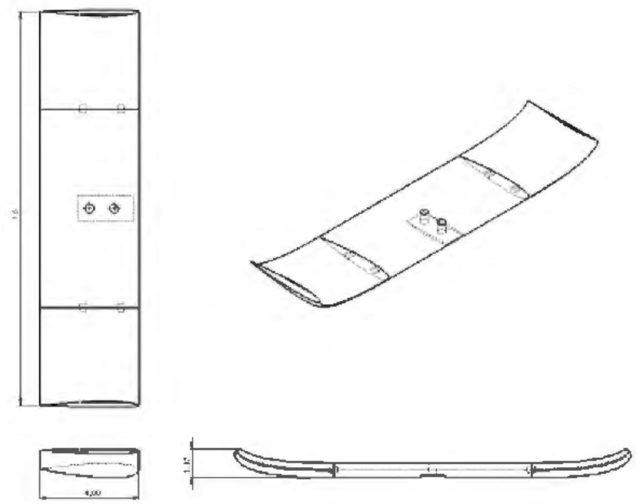

Figure 2: Drawing of current rear wing design

Rear Wing Span: 16" (406 mm)
Rear Wing Chord Length: 4" (102 mm)
Rear Wing Surface Area: $138in^2$ ($88890mm^2$)

Wing Material: PLA plastic core reinforced with carbon fibre epoxy composite
Fuselage Material: 6061-T6 Aluminum, 1" round bar
Mast Core Material: 6061-T6 Aluminum, 2" x ⅜" flat bar & PLA plastic core
Mast Skin Material: Carbon fiber epoxy layup

Wing Airfoil Profile: NACA 23015

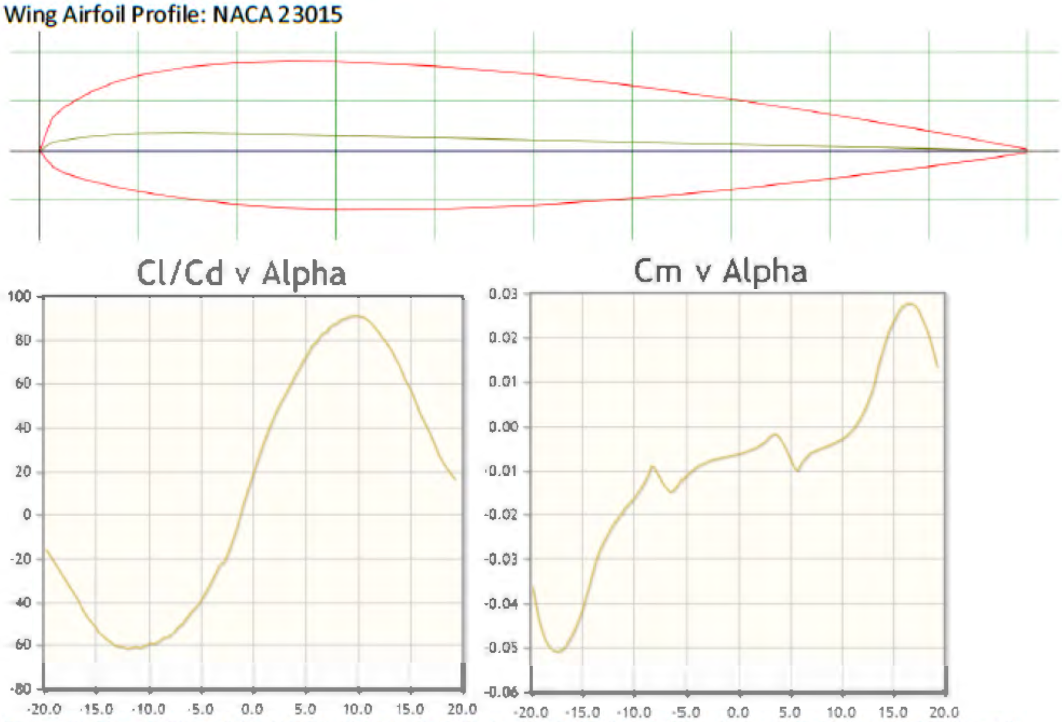

Figure 3: Top: Outline of the NACA 23015 airfoil. Bottom Left: Ratio of lift to drag coefficients as a function of attack angle. Bottom Right: Plot of the internal moment induced on the wing as a function of attack angle.

Figure C.2: Design review package (p2/9).

Lift Calculations

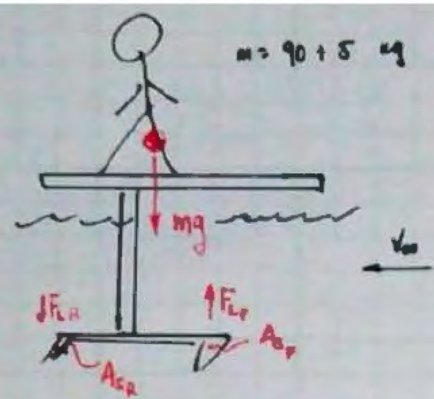

ASSUME RIDER + BOARD WEIGH $= W = mg$
$= (85+5)(9.81)$

→ NET REQUIRED LIFT $= \underline{932\ N}$

$$F_L = C_L \frac{\rho}{2} V^2 A_S \Rightarrow V = \sqrt{\frac{2F_L}{C_L \rho A_S}}$$

$$F_L = F_{LF} - F_{LR} \quad ; \quad A_S = A_{SF} - A_{SR}$$

PARAMETERS

SOURCE: AIRFOILTOOLS.COM

- NACA 23015
- ATTACK ANGLE, $\alpha = 0°$
- $Re = 1 \times 10^6$
- $C_L \approx 0.15$ (READ FROM "C_L vs α" GRAPH)

WATER @ 25°C, $\rho = 997\ kg/m^3$

$A_{SF} = 0.28309\ m^2$ (FRONT WING - T7)
$A_{SR} = 0.08889\ m^2$ (REAR WING - T2)
} $A_S = 0.19420\ m^2$

MINIMUM SPEED REQUIRED FOR LIFT: ($\alpha = 0°$)

$$V = \left[\frac{2F_L}{C_L \rho A_S}\right]^{1/2} = \left[\frac{2(932)}{(0.15)(997)(0.1942)}\right]^{1/2} = 8.0113\ \frac{m}{s}$$

$= 17.92$ mph

FOR ($\alpha = 1°$) ; $C_L \approx 0.24$

$$V = \left[\frac{2F_L}{C_L \rho A_S}\right]^{1/2} = \left[\frac{2(932)}{0.24(997)(0.1942)}\right]^{1/2} = 6.3335\ \frac{m}{s}$$

$= 14.167$ mph

FOR ($\alpha = 2°$) ; $C_L \approx 0.35$

$$V = \left[\frac{2(932)}{0.35(997)(0.1942)}\right]^{1/2} = 5.2447\ m/s$$

$= 11.732$ mph

Figure C.3: Design review package (p3/9).

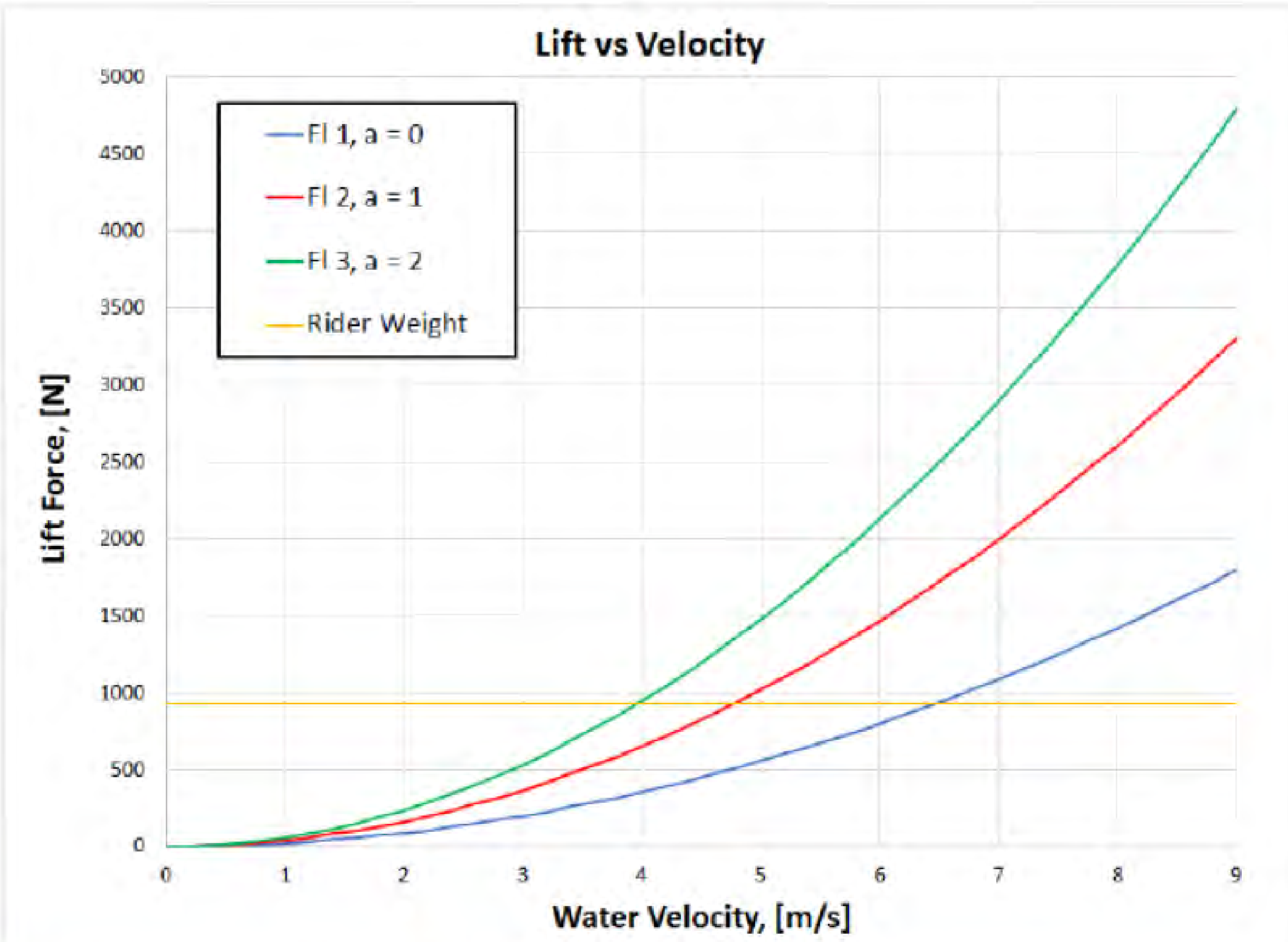

Figure 4: Plot showing the required lift (yellow line) and the lift generated by the NACA 23015 foil for three different attack angles, as a function of fluid velocity.

The above plot shows water velocity vs net lift force to be theoretically achieved by the surf foil. In green, red, and blue are shown the expected lift forces for different angles of attack, of 0, 1, and 2 degrees with respect to the direction of fluid flow. The yellow line indicates the minimum lift force required for the surf foil and rider to achieve equilibrium with gravity. The points at which the lift force curves intersect with this line indicates the minimum velocity required for hydrofoiling to occur.

A variety of attack angles were used to give more insight into the likely ranges of foiling velocities. Due to the variability in rider weight, surfing conditions, and riding style, the results presented above are theoretical and likely to change in practice. In particular, small changes in the angle of attack dramatically affect the amount of lift produced.

Figure C.4: Design review package (p4/9).

Competitive Analysis

Figure 5: Picture of the Slingshot Hover Glide kite foil

Figure 6: Cabrinha Double Agent hydrofoil

2019 Slingshot Hover Glide kite foil
(https://www.slingshotsports.com/2019-Hover-Glide-FKite-Foil)

Slingshot Features:
Large, low-aspect Space Skate 65 wing has tons of lift and stability
Dihedral shape provides “self-centering” flight
Shift Fuselage: Different connection points for different performance
Aluminum mast- sturdy, affordable super durable
Excellent wake and surf crossover
Safe-T winglets prevent injury
Stable 71cm (28 inch) mast

Cabrinha Double Agent Hydrofoil / Surf Skate
(https://www.cabrinhakites.com/products/double-agent)

Cabrinha Features:
Fun multi use board: foil / surf skate / wake surf
Easy to use and progress
Lively and responsive shape
Single concave to angled v-tail channels provides exceptional grip
Strapless, 2 or 3 strap configuration - for a fully customizable ride
Full EVA deck pad - thick & comfortable
TT quad fins for surf skate / wake surf use
Compatible with the modular HI:RISE foil system

Figure C.5: Design review package (p5/6).

Solidworks Model

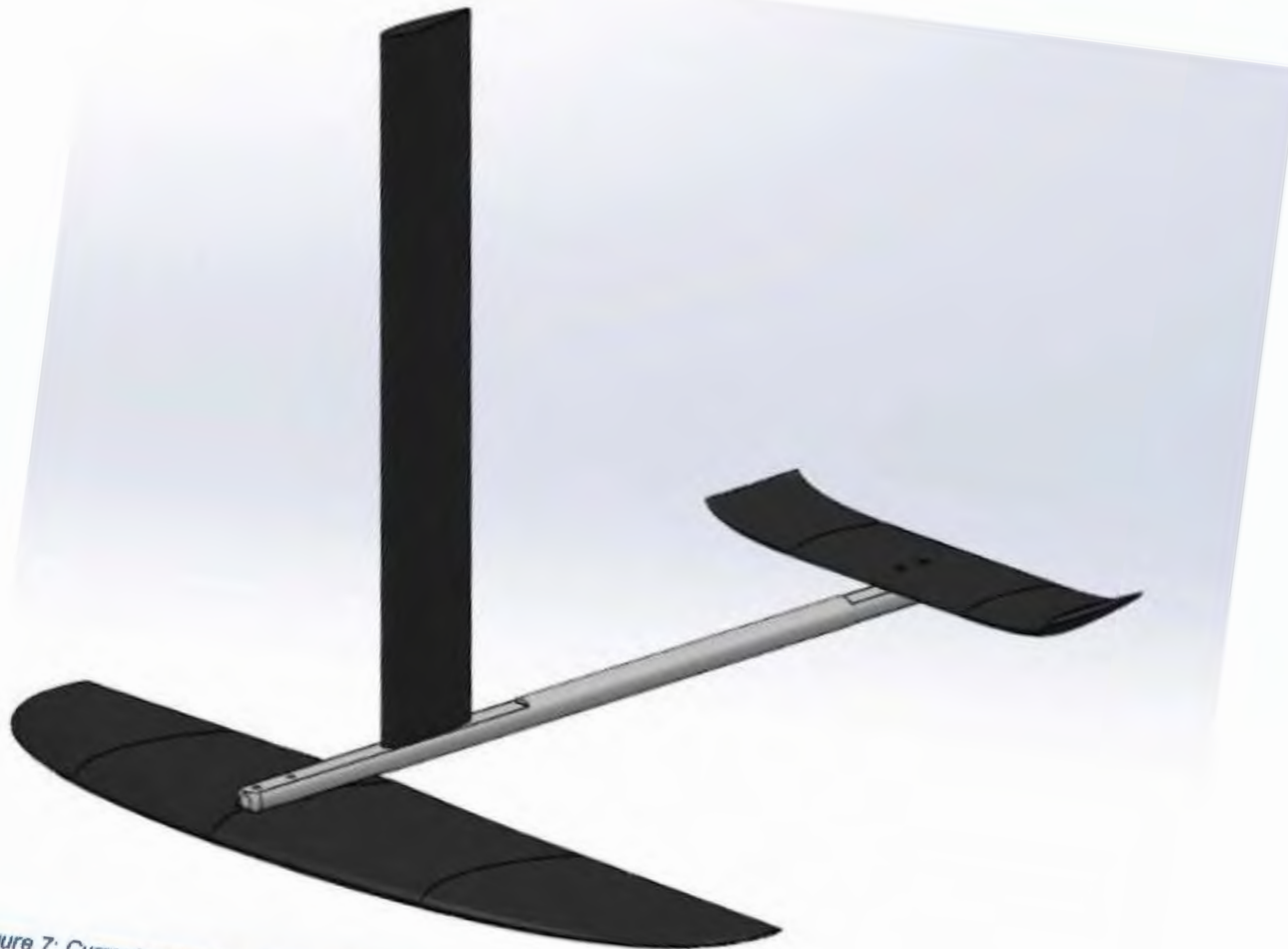

Figure 7: Current model of the hydrofoil design

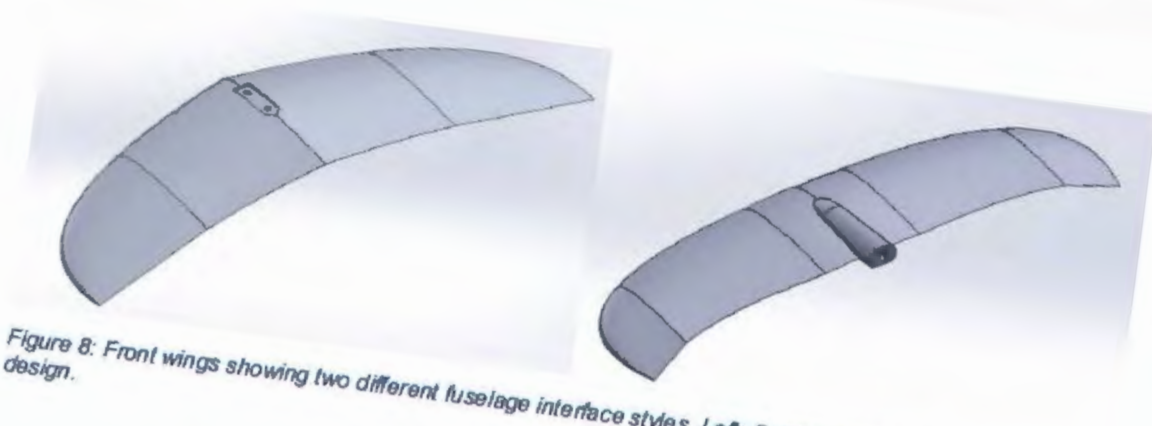

Figure 8: Front wings showing two different fuselage interface styles. Left: Current design. Right: Previous design.

Figure C.6: Design review package (p6/9).

Manufacturing & Prototyping Process

Front & Rear Wings

For the purpose of producing a test prototype, the hydrofoil wings wings are to be manufactured using 3D printing and carbon fiber epoxy composite. The complex wing geometry will be reproduced from CAD using filament deposition modelling (FDM). The material to be used is a plastic commonly used in FDM, polylactic acid (PLA). The wings must be 3D printed in sections due to print size and print orientational limitations. Once all wing sections are printed, they are to be assembled and fused together using a high strength epoxy.

The mounting holes on each wing will be reinforced with aluminum sheet metal and anti-crush inserts. This reinforcement assembly is to be epoxied in place onto the plastic PLA cores. The purpose of this reinforcement assembly is to prevent failure at the mounting location to the fuselage. This will allow the mounting hardware to be torqued sufficiently to ensure a rigid connection between the fuselage and wings.

The wings' surfaces will then be prepared for carbon fibre layup. A marine grade epoxy matrix is to be used with carbon fibre mats to create a structural composite material.

Fuselage

The fuselage will be manufactured by milling the ends of a 1" diameter 6061-T6 aluminum round bar. This will provide a smooth, flat surface for the interface between the wings and the fuselage. Holes are to be drilled and tapped on the flat surface to receive the bolts attaching the mast, front and rear wings. The leading and trailing faces are to be streamlined in order to reduce drag as well as providing a pleasing aesthetic to the fuselage.

Mast

The mast will be built around a 6061-T6 Aluminum 2" x ⅜" flat bar that runs the entire length of the mast. Exterior core components to form the desired fluid dynamic shape will be 3D printed using PLA. This will provide a consistent structure for the carbon fiber layup giving the mast the required strength and stiffness. Holes will be drilled and tapped to allow the mast to be mounted to the board pedestal and fuselage.

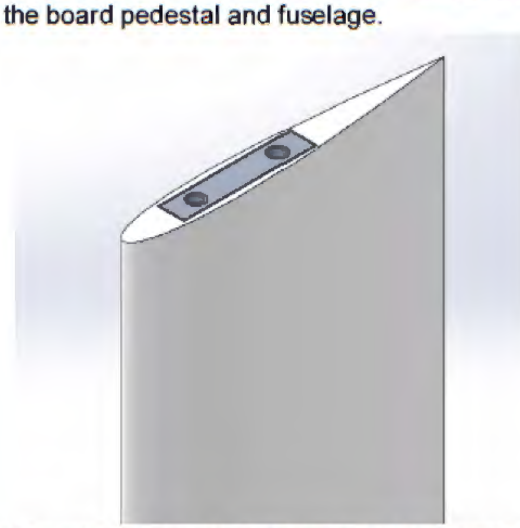

Figure 9: Solidworks model of the mast showing the 3D printed outer shape and the barstock core.

Figure C.7: Design review package (p7/9).

Schedule Status

The project schedule is being tracked using a Gantt chart. BTB Engineering is pleased with the current state of the schedule. All milestones to date have been completed. The virtual models of key components are nearly complete and material testing is underway. BTB Engineering is confident that the projected date of completion will coincide with the actual date of project completion.

Figure 10: Project Gantt chart

Cost Projections

The following list provides an itemized breakdown of the material costs required.

Surfboard: $800.00
Mounting Pedestal: $90.00
Materials for Mast: $50.00
Materials for Fuselage: $25.00
Materials for Front and Rear Wings: $75.00
Misc. Hardware: $30.00

Total: $1070.00

Figure C.8: Design review package (p8/9).

Project Risk Analysis

With the aid of our in-house plastics specialist, Greg King, all parts requiring carbon fibre epoxy composite will be fabricated using vacuum bag techniques.
Delamination due to air pockets introduced during the layup process are a concern and will be mitigated by using vacuum bagging all carbon fiber parts. After consultation with composites experts, the issue galvanic corrosion of aluminum in contact with carbon fiber has been brought to our attention and direct contact between these two materials will be mitigated by applying a anodizing to all aluminum parts.

Figure 11: Cabrinha pedestal for joining the mast to the board.

The pedestal (which joins the mast to the board) needs to be purchased and analysed in order to locate the mast attachment points, this creates a time concern which will be mitigated by ordering the pedestal within one week of the design review. Concerns about the attachment points between the wings and fuselage have been identified due to potential crushing during attachment and loading. One method to address this issue is to install anti-crush guards.

The fuselage provides the locating points for both wings and the mast. As highlighted in the Lift vs Velocity graph, small changes in the angle of attack have a significant impact on the amount of lift generated for a particular velocity. For this reason, the fuselage will require precise machining to ensure accurate rotational and hole alignment of the components. Additionally, shims will be manufactured to adjust the attack angle. The shims will be placed between the fuselage and mast as needed to adjust the attack angle.

Preliminary calculations show that the mast design will have minimal deflection under the expected operating conditions, however a more detailed analysis of the mast deflection will be conducted to include the 3D printed material and the carbon fiber skin.

Figure C.9: Design review package (p9/9).

Appendix D: Code for Processing NACA Profiles into SolidWorks Readable Filele File

```
/*****************************************************************************
Purpose: This program will accept NACA x and y points from
h ttp://airfoiltools.com/airfoil/naca4digit
and append a z column to it so that it can be opened as a curve in solidworks.
It can also generate a scaled wing profile.

#include <stdio.h>
#include <stdlib.h>
#include <math.h>
#include <string.h>
#pragma warning(disable:4996)
//---------------------------------- CONSTANTS ------------------------------------------
#define PI  3.14159265358979
#define MAX_ITERS 100000 // maximum iterations for F-D
#define MAX_RESIDUAL (1.0e-8) // solution accuracy
#define FILE_NAME "Foilpoints.txt"
#define ROWS  199
#define COLS  3
//------------------------ FUNCTION PROTOTYPES -----------------------------------
void calcFN();
//------------------------ CODED FUNCTIONS ------------------------------------------
// DESCRIPTION: Main function
// ARGUMENTS: none
// RETURN VALUE: return 0 to O/S to indicate normal termination
int main()
{
	int nodes; // counter variables
	double tFinal, *tNew, *tOld; //simulation variables
	calcFN();
	printf("Done\n");
	getchar();
	return 0;
}

// DESCRIPTION: Prints a NACA wing profile in a format that is compatible
// with solidworks
// ARGUMENTS:		none
// RETURN VALUE: none
void calcFN()
{
	int i, j;
	double *x, *y, *z;
```

```
char filef[50], file[50], filet[50];
FILE *f, *t, *p, *q;

// Dynamic memory allocation
x = (double*)malloc((double)ROWS * sizeof(double));
y = (double*)malloc((double)ROWS * sizeof(double));
z = (double*)malloc((double)ROWS * sizeof(double));

for (i = 0; i < ROWS-1; i++) // zero allocation for each axis
{
	x[i] = 0.0;
	y[i] = 0.0;
	z[i] = 0.0;
	//printf("%lf\n", x[i]); //For debugging
}

//Assign file name to array
sprintf(file, FILE_NAME);
//Open file streat to write
t = fopen(file, "r");

	for (j = 0; j < ROWS-2; j++)
	{
		fscanf(t,"%lf %lf",&x[j],&y[j]); //Reads data from the input file
	//	printf("%lf, %lf, %lf\n", x[j],y[j],z[j]); //For debugging
	}
fclose(t);

//Assign file name to array
sprintf(filef,"Foilpointscenter.txt");
//Open file streat to write
f = fopen(filef, "w");

for (i = 0; i < ROWS-2; i++) //Prints the coordinates for x, y, & z in columns
{
	fprintf(f, "%lf, %lf, %lf\n ", SF*x[i], SF*y[i], z[i]);
}
fclose(f);

// Commented out because we an used blocks in Solidworks to scale the wings
/*
//Assign file name to array
sprintf(filet, "Foilpointsend.txt");
//Open file streat to write
```

```
        p = fopen(filet, "w");
        for (i = 0; i < ROWS - 2; i++)
//Prints a scaled coordinate set for the wing profile
        {
                fprintf(p, "%lf, %lf, %lf\n ", x[i],y[i],z[i]);
        }
        fclose(p);

        //Assign file name to array
        sprintf(filet, "Foilpointxz.txt");
        //Open file streat to write
        q = fopen(filet, "w");
        for (i = 0; i < ROWS - 2; i++)
//Prints the wing profile coordinates in the xz plane
        {
                fprintf(q, "%lf, %lf, %lf\n ", x[i], z[i], y[i]);
        }
        printf("\nIt works!\n");
        fclose(q);
        */
}
```

Appendix E: Crush Protection Calculation for M8

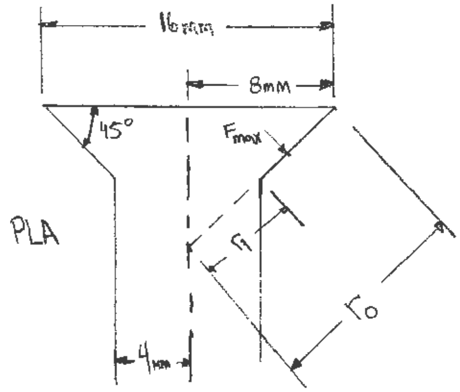

$\sigma_{yield} = \sigma_y = 26.0 \text{ MPa} = 3770 \text{ psi}$

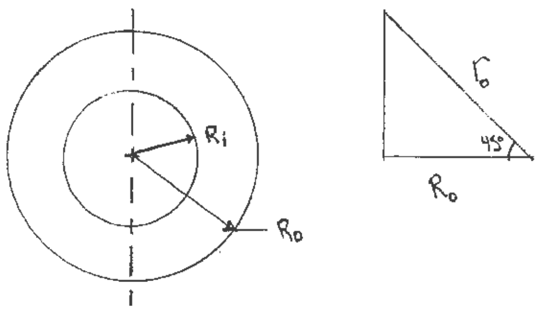

$R_o = 8mm \quad , \quad R_i = 4mm$

$r_o = \sqrt{R_o^2 + R_o^2} = \sqrt{8mm^2 + 8mm^2}$

$r_o = 11.314 \text{ mm}$

$r_i = 5.6569 \text{ mm}$

$A_{surface} = A_s = \pi\left(r_o^2 - r_i^2\right) = \pi\left(11.314mm^2 - 5.6569 mm^2\right) = 301.59 mm^2$

$\sigma = \frac{F}{A} \quad , \quad F = \sigma A$

$F_{max} = \sigma_y \cdot A_s = 26.0 \frac{N}{mm^2} \cdot 301.59 mm^2 = 7841.3N$

Max allowable force: $F_{max} = 7840N = 1760 lb$

$F_{Lift} = 1310N$

Safety Factor for lift $= \frac{7840N}{1310N} = 5.98$ $\quad SF_{Lift} = 5.98$

Figure E.1: Wing compressive stress calculations. Based on M8 - Flat Head Screw

Appendix F: Fuselage Length Calculations

Fuselage length calculations:

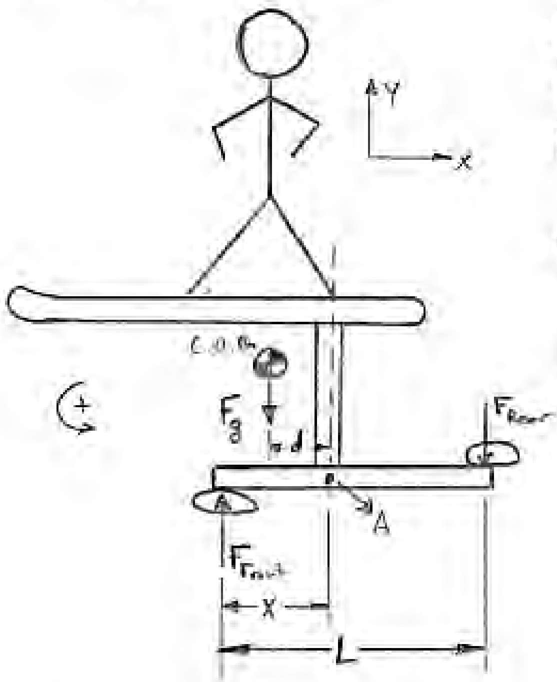

F_g = Force of gravity due to rider & board

F_{Front} = Lift force of front wing

F_{Rear} = Lift force of rear wing

L = Distance between lift forces

d = Distance between center of gravity & mast

X = Distance from mast to front lift force lengthwise

$$\sum F_y = \emptyset \rightarrow F_{Front} - F_g - F_{Rear} = \emptyset \rightarrow F_g = F_{Front} - F_{Rear}$$

$$\sum M_A = \emptyset \rightarrow F_g d - F_{Front}(x) - F_{Rear}(L - x) = \emptyset$$

$$X = \frac{(F_{Front} - F_{Rear})d - F_{Rear}L}{F_{Front} - F_{Rear}}$$

Assuming at lift velocity,

$F_g = 931.99N$ $F_{Front} = 1306.42N$ $F_{Rear} = 374.43N$

$d = 15.25$ in $L = 26.5$ in

Then,

$X = 4.6036$ in

Figure F.1: Fuselage length calculations

Appendix G: Fuselage As-Built Shop Drawing

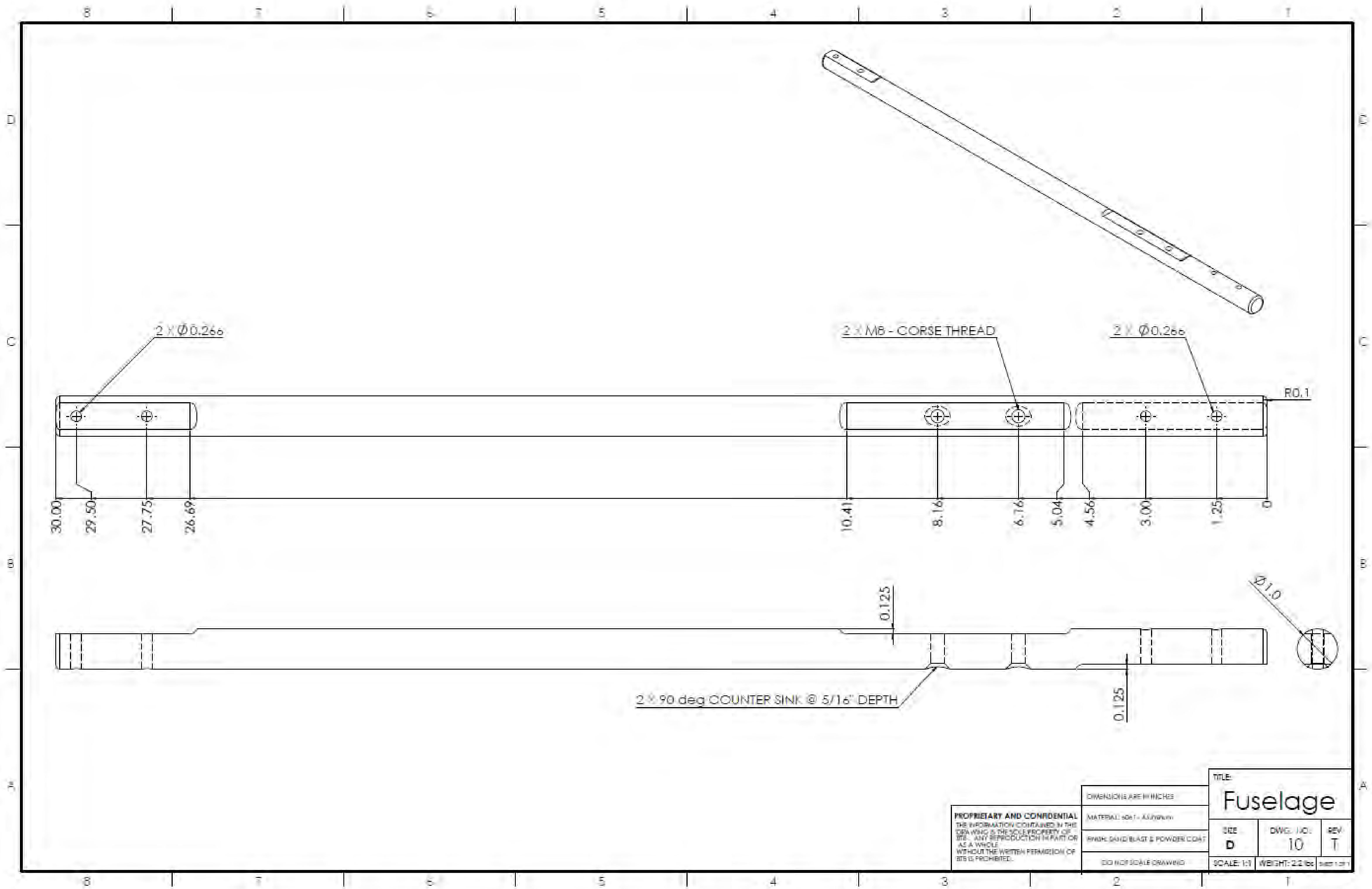

Figure G.1:Fuselage as-built shop drawing.

Appendix H: Fuselage Stress Calculations

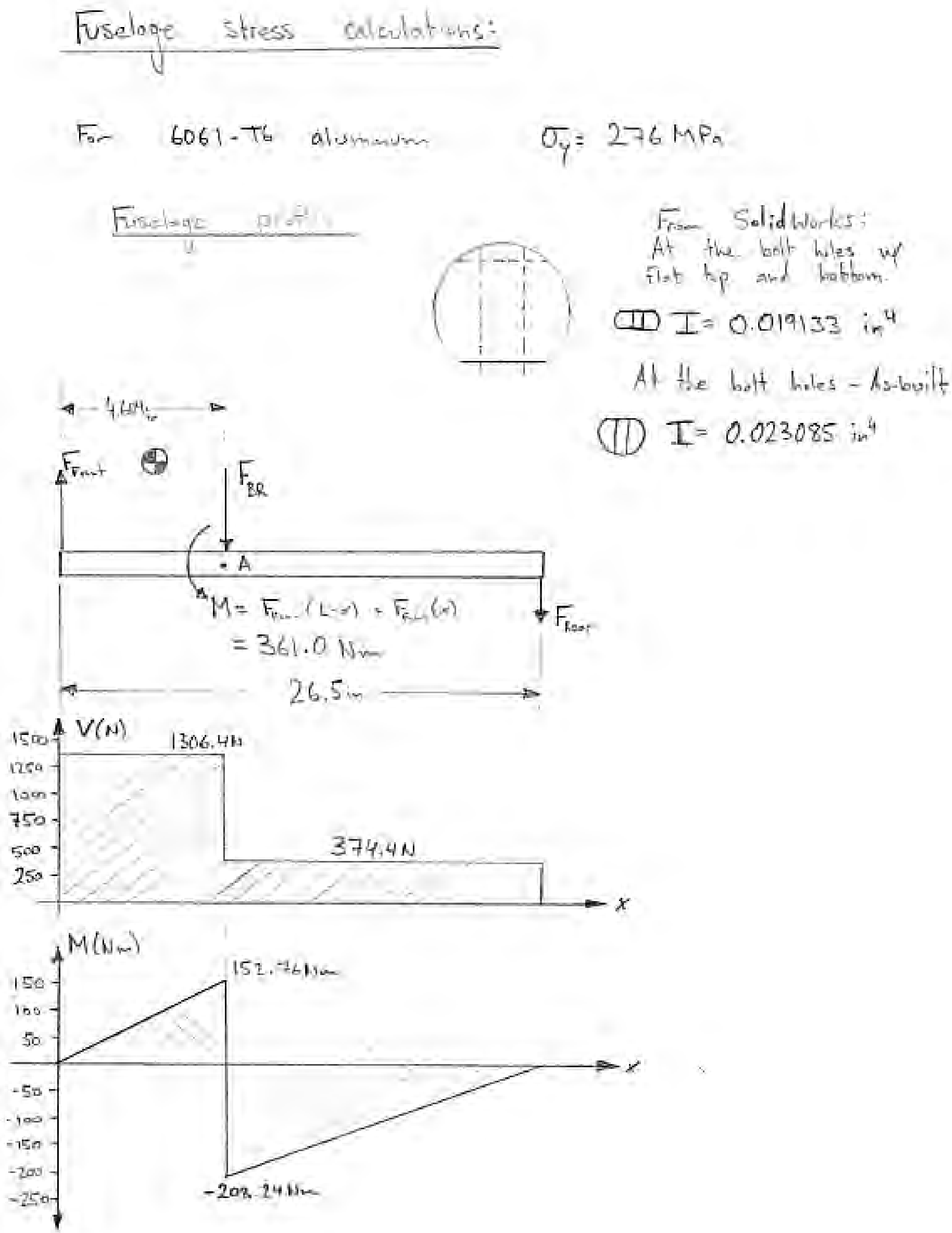

Figure H.1: Fuselage stress calculations (p1/2).

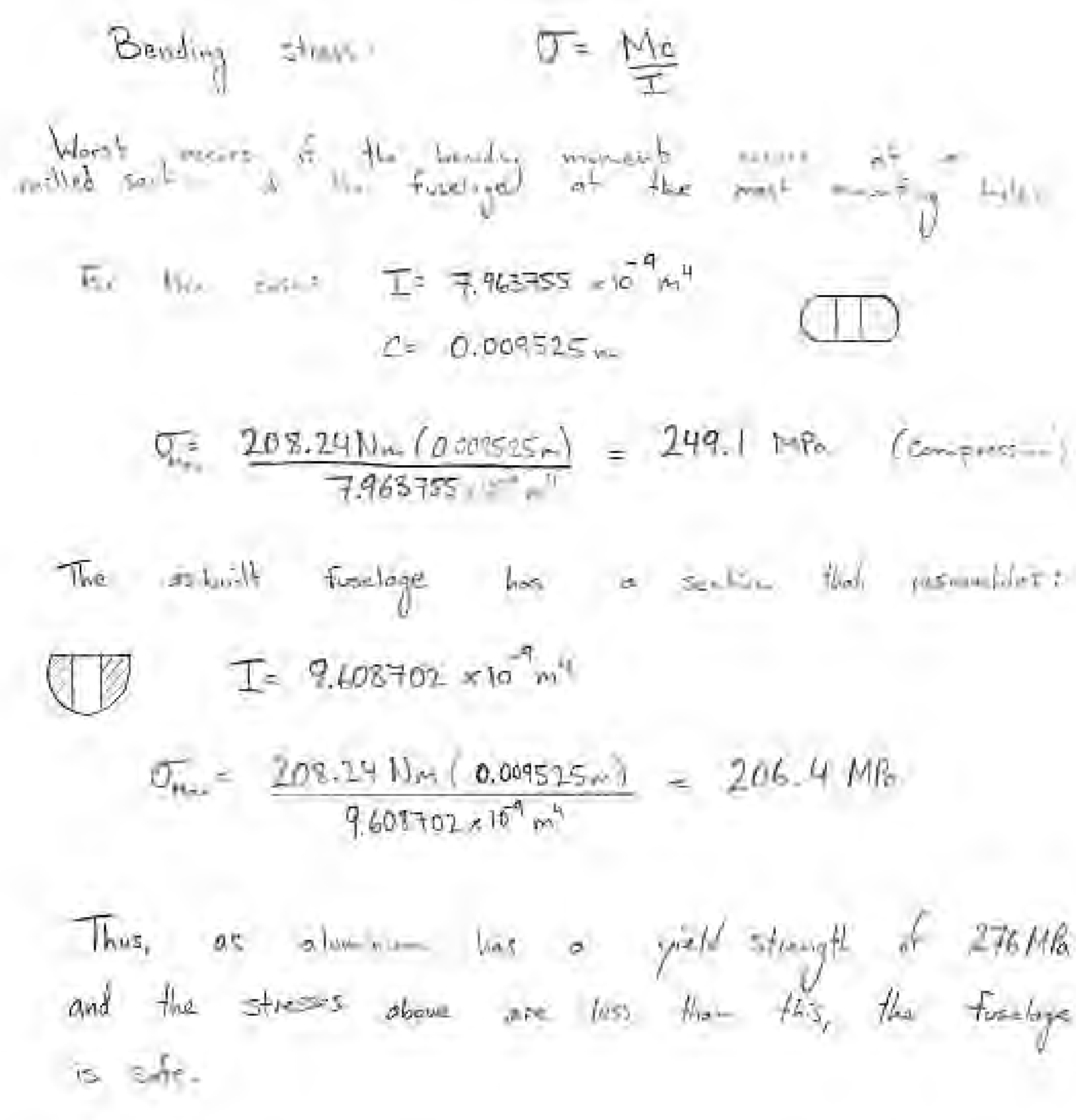

Bending stress: $\sigma = \frac{Mc}{I}$

Worst case occurs if the bending moment occurs at a milled slot in the fuselage at the most mounting holes.

For this case: $I = 7.963755 \times 10^{-9}\ m^4$

$c = 0.009525\ m$

$$\sigma_{max} = \frac{208.24\ Nm\ (0.009525\ m)}{7.963755 \times 10^{-9}\ m^4} = 249.1\ MPa \quad \text{(Compression)}$$

The as-built fuselage has a section that resembles:

$I = 9.608702 \times 10^{-9}\ m^4$

$$\sigma_{max} = \frac{208.24\ Nm\ (0.009525\ m)}{9.608702 \times 10^{-9}\ m^4} = 206.4\ MPa$$

Thus, as aluminum has a yield strength of 276 MPa and the stresses above are less than this, the fuselage is safe.

Figure H.2: Fuselage stress calculations (p2/2).

Appendix I: Project Gantt Chart

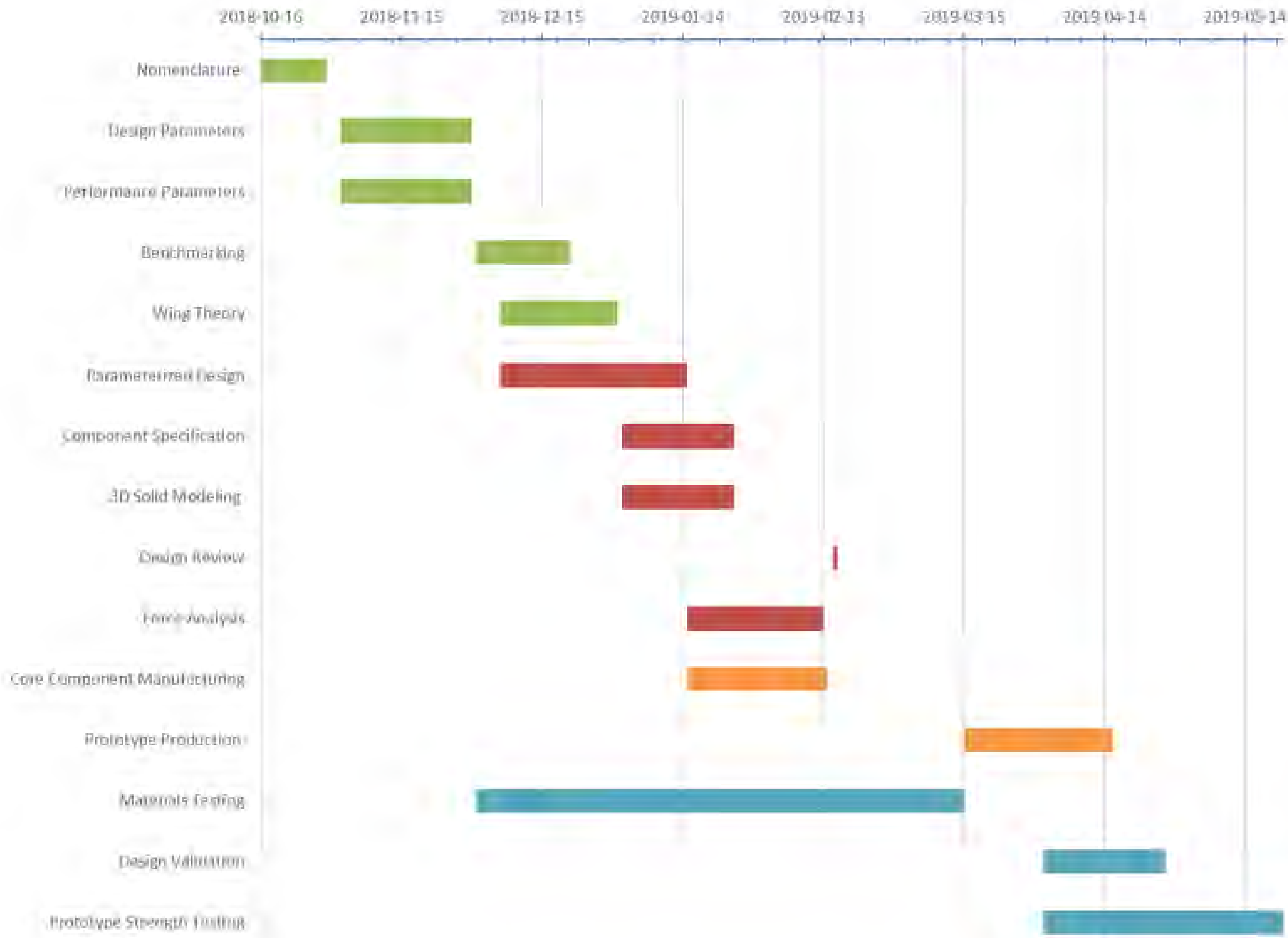

Figure I.1: Project Gantt chart.

Appendix J: Front Wing Drawings & Dimensions

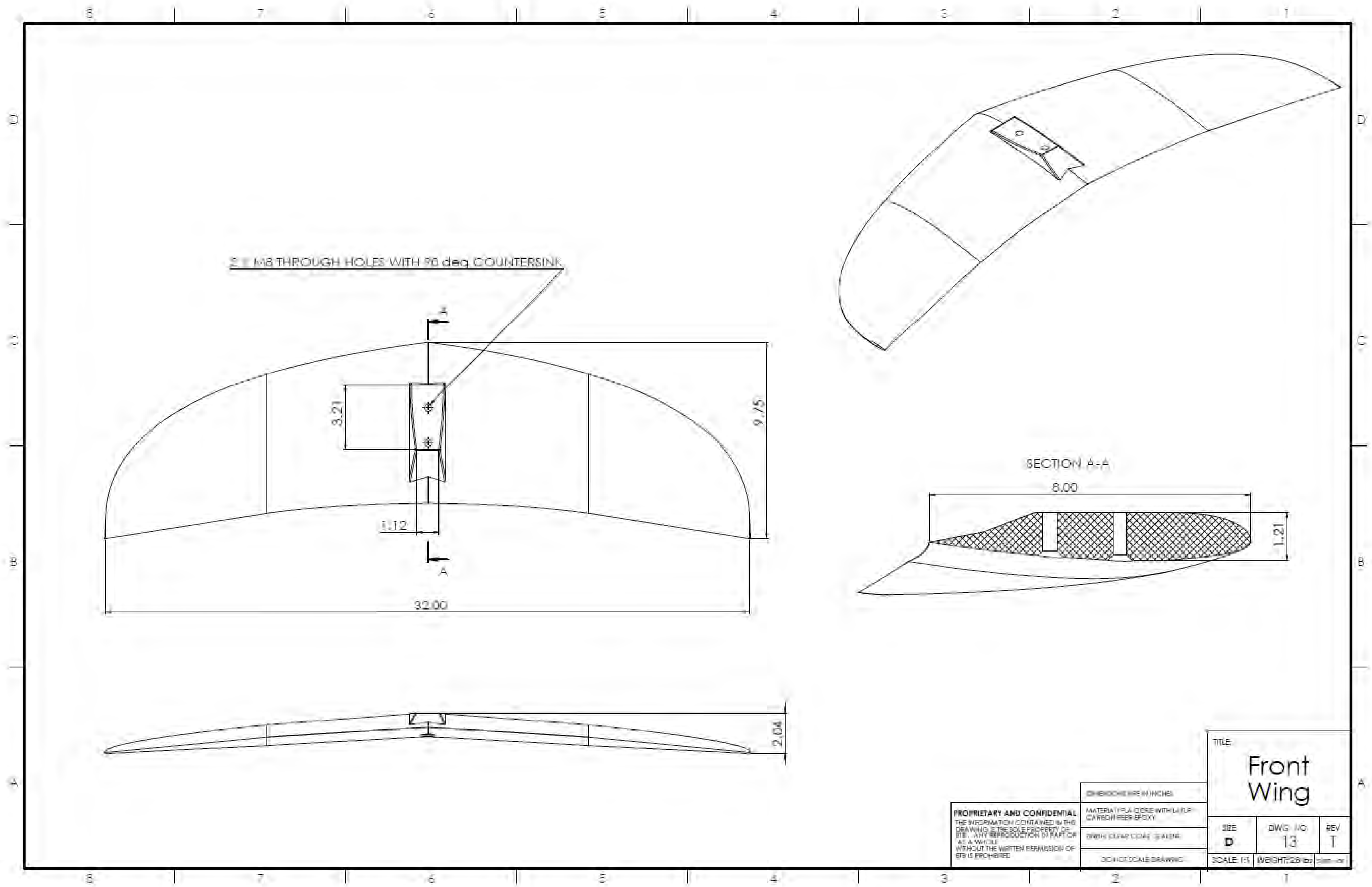

Figure J.1: Front wing CAD drawing

Appendix K: Front Wing Drawings & Dimensions

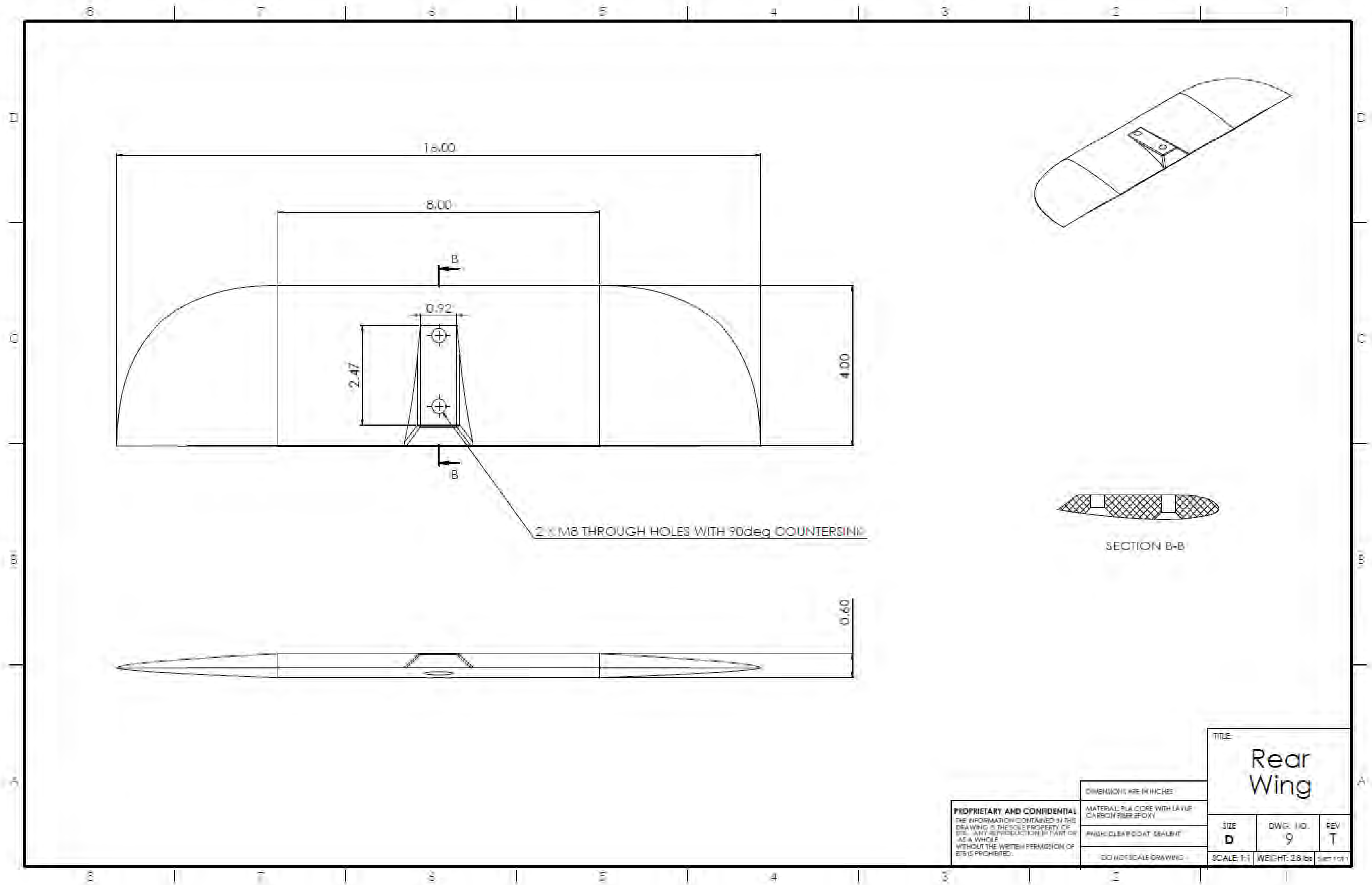

Figure K.1: Rear wing CAD drawing.

Appendix L: Responsibility Assignment Matrix

Responsibility Assignment Matrix	Stakeholder					
	Jackson Bryla	**Todd Backus**	**Anthony Taylor**	**Johan Fourie**	**Greg King**	**Poseidon Adventures**
Role	Chief Engineer	Lead Manufacturing Engineer	Lead Materials Engineer	Technical Advisor	Manufacturing & Materials Advisor	Project Sponsor
Activity						
Theory & Nomenclature	A	R	R	C	I	I
Design Parameters	R	A	R	C	I	I
Performance Parameters	R	R	A	C	I	I
Benchmarking	R	A	R	I	C	I
3D Modelling	A	R	R	I	I	I
Force Analysis	R	R	A	C	I	I
Component Specification	A	R	R	I	C	I
Design Review	A	R	R	C	C	C
Core Components	R	R	A	I	C	I
Composite Lay-up	R	A	R	I	C	I
Assembly	R	A	R	I	C	I
Prototype Manufacture	R	A	R	C	C	I
Materials & Strength Testing	R	R	A	I	I	I
Design Validation	A	R	R	C	I	I
Legend	**A = Accountable**	**R = Responsible**		**C = Consult**	**I = Inform**	

Figure L.1: Project responsibility assignment matrix.

Appendix M: Project Work Breakdown Structure

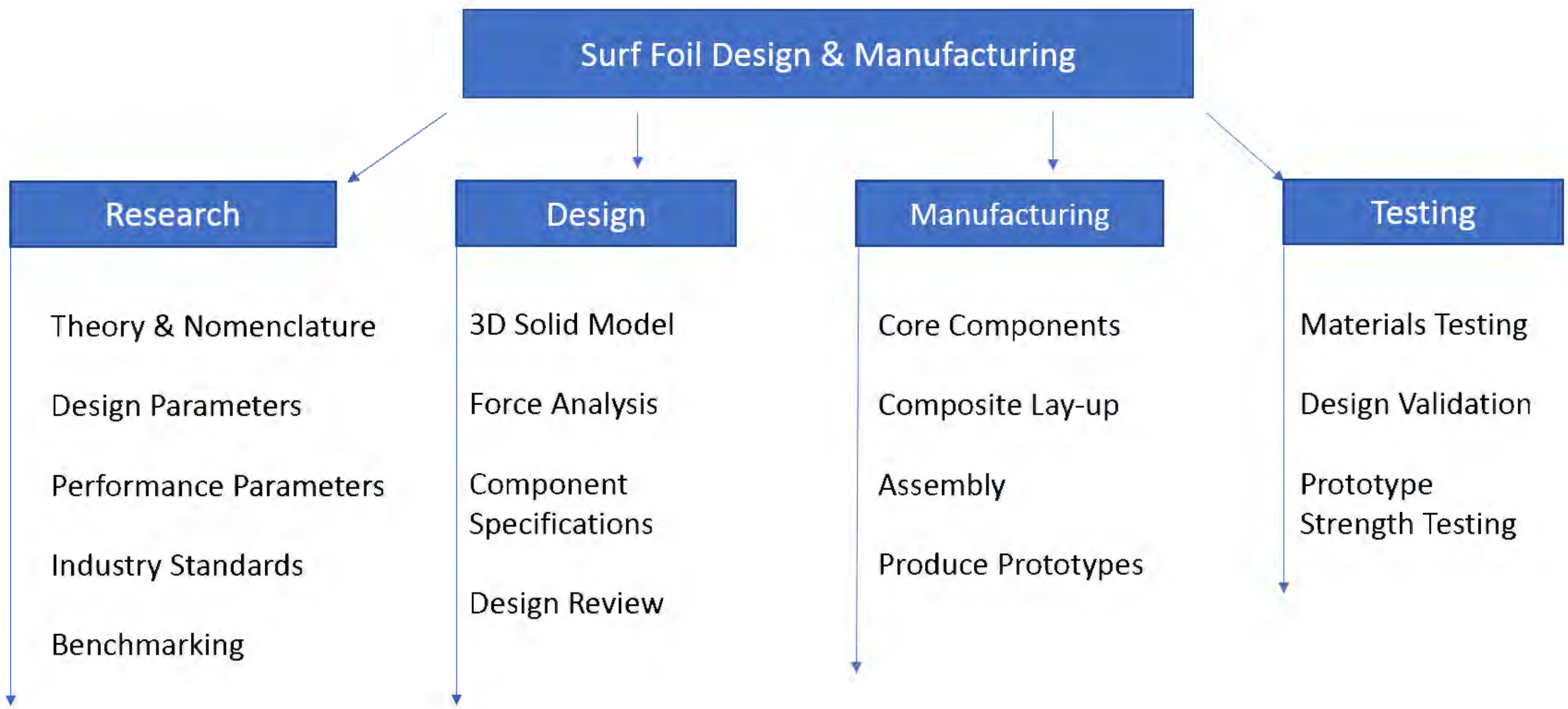

Figure M.1: Work breakdown structure chart for the project.

Appendix N: Milestone Schedule: Key Dates of Projected Milestone Schedule

Table N.1: Project Milestone Schedule Key Dates.

Task	End Date
Complete Research	November-30-18
Design & 3D Solid Model	January-14-19
Design Review	February-15-19
Manufacture Prototype	May-01-19
Technical Analysis Report	May-01-19
Project Wrap-up	May-20-19